

Adverse Weather Scenarios for Future Electricity Systems: Developing the dataset of short-duration ramping events

Author(s): Isabel Rushby, Megan Pearce and Dr Laura Dawkins

Reviewed by: Dr Emily Wallace

Prepared for: National Infrastructure Commission

Version: 10, March 2022

If printing double-sided you will need this blank page. If printing single sided, please delete this page

Disclaimer

- This document is published by the Met Office on behalf of the Met Office on behalf of the Secretary of State for Business, Energy and Industrial Strategy, HM Government, UK. Its content is covered by © Crown Copyright 2022.
- This document is published specifically for the readership and use of National Infrastructure Commission and may not be used or relied upon by any third party, without the Met Office's express written permission.
- The Met Office aims to ensure that the content of this document is accurate and consistent with its best current scientific understanding. However, the science which underlies meteorological forecasts and climate projections is constantly evolving. Therefore, any element of the content of this document which involves a forecast or a prediction should be regarded as our best possible guidance, but should not be relied upon as if it were a statement of fact. To the fullest extent permitted by applicable law, the Met Office excludes all warranties or representations (express or implied) in respect of the content of this document.
- Use of the content of this document is entirely at the reader's own risk. The Met Office makes no warranty, representation or guarantee that the content of this document is error free or fit for your intended use.
- Before taking action based on the content of this document, the reader should evaluate it thoroughly in the context of his/her specific requirements and intended applications.
- To the fullest extent permitted by applicable law, the Met Office, its employees, contractors or subcontractors, hereby disclaim any and all liability for loss, injury or damage (direct, indirect, consequential, incidental or special) arising out of or in connection with the use of the content of this document including without limitation any and all liability:
 - relating to the accuracy, completeness, reliability, availability, suitability, quality, ownership, non-infringement, operation, merchantability and fitness for purpose of the content of this document;
 - relating to its work procuring, compiling, interpreting, editing, reporting and publishing the content of this document; and
 - resulting from reliance upon, operation of, use of or actions or decisions made on the basis of, any facts, opinions, ideas, instructions, methods, or procedures set out in this document.
- This does not affect the Met Office's liability for death or personal injury arising from the Met Office's negligence, nor the Met Office's liability for fraud or fraudulent

misrepresentation, nor any other liability which cannot be excluded or limited under applicable law.

- If any of these provisions or part provisions are, for any reason, held to be unenforceable, illegal or invalid, that unenforceability, illegality or invalidity will not affect any other provisions or part provisions which will continue in full force and effect.

Contents

Disclaimer	3
Contents	5
Executive Summary	6
1 Introduction	8
2 Summary of Phase 3a: Characterising short-duration ramping events	10
2.1 Defined regions.....	11
3 Developing the dataset of short-duration adverse weather scenarios (ramping events) for future electricity systems.....	13
3.1 Data source	13
3.1.1 UK Climate Projections 2018 (UKCP18)	13
3.2 Data calibration.....	15
3.2.1 Bias correction of 10m wind speed	16
3.2.2 Representing 100m wind speed.....	17
3.3 Exploring adverse weather scenarios in Euro4 and UKCP18.....	21
3.4 Statistical extreme value analysis to quantify adverse weather in different climates	27
3.5 Selecting adverse weather scenarios for the final dataset.....	44
4 The Adverse Weather Scenarios for Future Electricity Systems dataset	46
4.1 Existing available dataset (long-duration events)	46
4.2 Updates to the dataset (short-duration events)	46
4.3 Downloading the data	46
5 Summary and Conclusion	51
6 References	54
7 Glossary	56
8 Appendix.....	57

Executive Summary

The first National Infrastructure Assessment (National Infrastructure Commission, 2018), published by the National Infrastructure Commission (the Commission) in 2018, recommends targeting a transition of the UK electricity system to a highly renewable generation mix, incorporating increasing wind and solar power capacities. This is consistent with a number of other recent reports such as the Climate Change Committee's Sixth Carbon Budget report (Climate Change Committee, 2020), and the International Energy Agency's Net Zero by 2050 Roadmap for the Global Energy Sector (International Energy Agency, 2021), all reflecting the need for a de-carbonised energy system to help tackle the climate crisis.

Whilst desirable, transitioning to this highly renewable mix will increase the vulnerability of the UK's electricity system to adverse weather conditions, such as sustained periods of low wind speeds leading to low wind generation, coupled with cold winter or high summer temperatures leading to peak electricity demand, or short-duration changes in wind speed or solar radiation that can result in rapid, instantaneous changes in generation. Consequently, the Commission want to improve understanding of the impact of adverse weather conditions on a highly-renewable future system. This will support the recommendations it makes to government and provide beneficial inputs to those that model and design future electricity systems.

To improve this understanding, the Met Office have been working with the National Infrastructure Commission and Climate Change Committee to develop two datasets of adverse weather scenarios, based on physically plausible weather conditions, representing a range of possible extreme events, and the effect of future climate change. These datasets will allow for proposed future highly renewable electricity systems to be stress tested to evaluate resilience to challenging weather and climate conditions. The first of these datasets, published to the Centre for Environmental Data Analysis (CEDA) archive¹ in June 2021, focuses on long-duration adverse weather scenarios and characterises winter-time and summer-time wind-drought-peak-demand events, and summertime surplus generation events, in the UK and in Europe.

This report presents the development of the second dataset - short-duration adverse weather scenarios, characterising wind ramping events in the UK. It contains gridded daily average meteorological data (100m wind speed) associated with a range of examples of such events, capturing various extreme levels (1 in 2, 5, 10, 20, 50 and 100 year return period events) representative of present day.

¹ <https://catalogue.ceda.ac.uk/uuid/7beeed0bc7fa41feb10be22ee9d10f00>

The sensitivity of these short-duration adverse weather scenarios to climate change (specifically rising global temperatures) is explored. In support of findings of the previous phase of this work; in a UK system with high wind renewable capacity, sensitivity of the system to changing climate is small. Therefore, the data provided can be used to represent future weather conditions, as well as the present day.

The dataset is freely available to download from the Centre for Environmental Data Analysis archive, and a brief how-to guide for downloading the data is included at the end of this report.

The resulting short-duration subset of the 'Adverse Weather Scenarios for Future Electricity Systems' dataset can be used to test the resilience of a range of potential future electricity systems to large, short-term fluctuations in weather. This will enable energy system decision makers to support the security of energy supply as the UK becomes net-zero.

1 Introduction

The Met Office are developing a dataset of adverse weather events that can be used by energy system modellers to test the weather and climate resilience of potential future highly renewable electricity systems. To date, the project has involved; an initial literature review (Dawkins, 2019), a project scoping report (Butcher and Dawkins, 2020), the characterisation of long-duration adverse weather stress events (Dawkins and Rushby, 2021) and the development of the ‘Adverse Weather Scenarios for Future Electricity Systems’ dataset of long-duration events (Dawkins et al., 2021a) and associated report (Dawkins et al., 2021b). The most recent phase has extended this work to characterise short-duration adverse weather stress events (Pearce et al., 2021) and this report presents the development of the Adverse Weather Scenarios for Future Electricity Systems’ dataset of short-duration events.

Short-duration adverse weather scenarios are characterised by a large change in energy generation in a small time-window, known as ramping events. Specifically, a wind ramping event is characterised by large changes in wind speed, and subsequent wind power production, during a short time window. Similar to the long-duration dataset, the aim is to provide gridded meteorological data that represent wind ramping events for the UK, at various extreme levels (1 in 2, 5, 10, 20, 50 and 100 year return period events), and representative of a range of climate warming levels (current day, 1.5°C, 2°C, 3°C and 4°C above pre-industrial levels).

The method for characterising the short-duration events in the historical record has been developed using the Euro4 hindcast dataset (Pearce et al., 2021). However, this may only capture a narrow range of plausible weather conditions, and will not represent how such events may change in future climates. Therefore, this report presents the application of this method to the UK Climate Projections 2018 (UKCP18) (Lowe et al., 2018), to provide alternative realisations of the historical period 1981-2000, and hence additional plausible weather conditions, and to investigate how weather is likely to change in the future as a result of climate change. The adverse weather scenarios identified in these two data sources are used in combination within a non-stationary statistical extreme value analysis (EVA) to quantify the likelihood (i.e. the return period) of events, and how these may change in future warmer climates. The results of this analysis are then used to pick relevant adverse weather scenarios from the UKCP18 dataset, to be used to represent the various required extreme levels and warming levels within the final dataset. As the UKCP18 data is derived from a climate model, methods to validate and calibrate the data have been applied where necessary. This ensures, for example, that the climate model data is not too windy on average. Specifically, a univariate

variance scaling approach is used to bias correct the model data, and data science generalised additive models are developed to estimate 100m (above ground) wind speed from 10m wind speed.

This report firstly summaries the approach developed for characterising short-duration adverse weather scenarios, as previously published in Pearce et al. (2021). The method for creating the final dataset of short-duration adverse weather scenarios for future electricity systems is then presented. Initially, the climate model dataset (UKCP18) is introduced, and the methods for calibrating and imputing them are described. The adverse weather scenarios identified in the two data sources (Euro4 hindcast and UKCP18) are then compared and explored. Following this, the statistical EVA method used to quantify the likelihood of adverse weather scenarios in different climates is presented, and the approach used to select relevant periods of adverse weather for the final dataset, based on this analysis, is given. Finally, a full specification of the final 'Adverse Weather for Future Electricity Systems' dataset is provided, along with a brief how-to guide on how to download the dataset from the Centre for Environmental Data Analysis (CEDA) archive.

2 Summary of Phase 3a: Characterising short-duration ramping events

The Phase 3 (a) report (Pearce et al., 2021) presents the approach for characterising short-duration adverse weather events using meteorological data, focusing on ramping events associated with wind and solar renewable energy. It was found that the methods used to identify solar ramping events did not pick out ramps associated with meteorological changes, rather the diurnal cycle of solar radiation were picked out. Since these ‘ramps’ are highly predictable and do not represent high impact events the analysis of solar ramps was not continued in this report. The approach described in the Phase 3(a) report draws on the previous methods developed in Phase 2 of the project in combination with those explored in Cannon et al. (2015). A wind ramping event is characterised by large changes in wind speed, and subsequent capacity factor and hence wind power production, during a short time window.

The capacity factor defines, for a given time period, the ratio of actual generation compared to the maximum potential generation. When the wind speed is slower the capacity factor decreases i.e., there is a reduction in the potential for generation. The capacity factor is also impacted by the choice of wind turbine and its associated power curve. Whilst a ramping event can be identified by a rapid change in *generation*, it is possible to use the change in *capacity factor* to represent the generation change. This is because these quantities are proportional to each other (generation = capacity factor x installed renewable capacity). Similar to Cannon et al. (2015), this phase utilises changes in capacity factor to characterise short-duration adverse weather stress events (i.e. ramping events).

Below is a brief overview of the steps in the Phase 3 (a) approach to give context for the reference of some methods in Phase 3 (b). Please refer back to the Phase 2 (a) and Phase 3 (a) report for further detail on the method development (Dawkins and Rushby, 2021; Pearce et al., 2021).

Steps in the Phase 3 (a) approach:

1. Estimate wind electricity capacity factor in each grid cell by applying the wind turbine power curve to bias corrected Euro4 100m wind speed and aggregate for defined regions for onshore and offshore wind (see Section 2.1 for region detail).
2. Calculate change in capacity factor over time windows, defined as ‘for a given time window e.g., 3 hours and region e.g. Scotland, the number of times ‘maximum capacity factor change’ surpasses a particular change threshold. This is then used to determine the average number of ramping events per year that surpass each change threshold of interest for a given time window. The time windows explored are those used by Cannon et al. (2015): 1 hour, 3 hours, 6 hours, 12 hours and 24 hours. Due to the daily

reinitialisation of the models underlying the Euro4 data, 1 and 3 hour time windows containing midnight are excluded from the analysis.

3. For each time window and region, an *empirical* EVA is carried out to contextualise the extremity of ramping events, particularly focusing on the most extreme events. This *empirical* (i.e., based on the ranking of events observed in the 36-year Euro4 data record rather than fitting a statistical model) EVA identifies the observed *return period* (number of years in between events) of ramping events of a given *return level* (extremity of 'change in capacity factor'). This method was used to identify 1 in 2, 5, 10, 20 and 30-year return period wind ramping events for each region and time window combination.

This method was applied to 36 years of historical (1979-2014) meteorological data taken from the Euro4 hindcast dataset, and the resulting adverse weather events within the historical report were presented. Phase 3 utilises Euro4 hindcast data, which provides a much higher spatial resolution (4 km) representation compared to the ERA5 reanalysis dataset (30 km) used in Phase 2, to better capture the smaller scale meteorological conditions relevant for energy ramping events. For reference, the hourly Euro4 hindcast data was generated by the Met Office using the European Atmospheric Hi-Res² forecasting model, driven by ERA-Interim reanalysis data, to create a downscaled hindcast (i.e. a historical forecast) dataset.

2.1 Defined regions

An overview of the project regions defined in Phase 3 (a) and utilised in Phase 3 (b) are provided below, and shown in Figure 1.

For onshore wind there are three regions: Scotland (blue), East England (green) and West England and Wales (red), which were defined based on long-term climatology of mean annual 100m wind speed across the region. These are referred to within this report as 'Onshore North', 'Onshore East' and 'Onshore West'. Offshore wind has been handled independently of onshore wind and separated into a north (orange) and south (purple) region following insights from the project advisory group. These are referred to within this report as 'Offshore North' and 'Offshore South'.

²

https://www.metoffice.gov.uk/binaries/content/assets/metofficegovuk/pdf/data/european_model_data_sheet_lores1.pdf (Accessed: 14th December 2021)

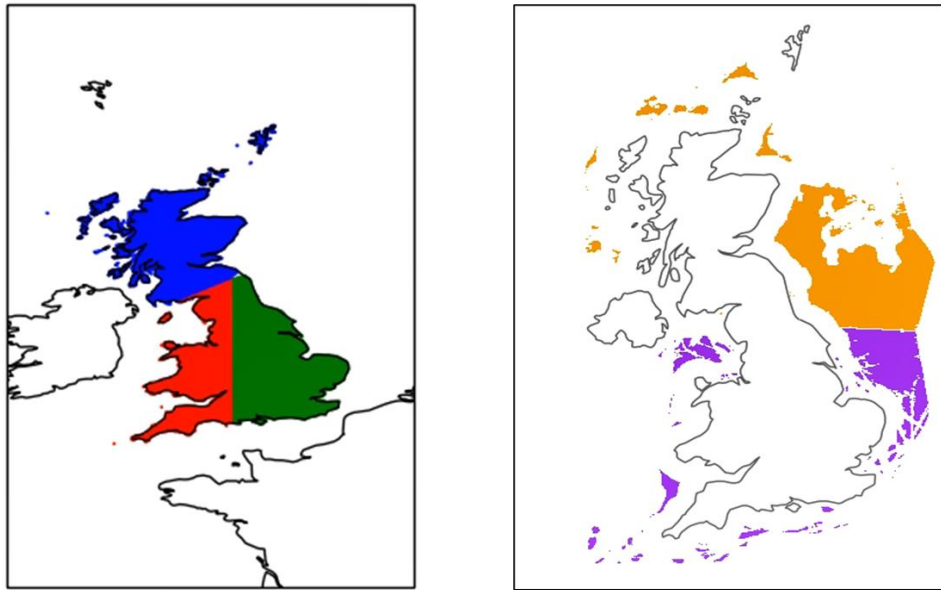


Figure 1: (a - Left) Defined project regions for Onshore wind: Scotland (blue), East England (green) and West England and Wales (red), and (b - Right) Defined project regions for offshore wind: offshore north (orange) and offshore south (purple).

3 Developing the dataset of short-duration adverse weather scenarios (ramping events) for future electricity systems

As highlighted in the ‘Weather and Climate Related Sensitivities and Risks in a Highly Renewable UK Energy System’ literature review (Dawkins, 2019) and the previous phase report ‘Adverse Weather Scenarios for Future Electricity Systems: Developing the dataset of long-duration events’ (Dawkins et al., 2021), a limitation of many electricity system studies is the use of the relatively short historical observed record of meteorological data. In using this observed record only, natural climate variability and anthropogenic climate change are not adequately captured, which may lead to the under- or over-estimation of plausible extreme stress on the electricity system. That is, it may be physically plausible to observe a weather event more extreme than that experienced in the historical record, but that it just hasn’t been observed within the limited record. Further, future global warming is likely to impact electricity system relevant meteorological variables, particularly temperature, which could lead to a change in the extremity of adverse weather scenarios.

To better capture alternative plausible weather conditions and anthropogenic climate change within the final dataset of short-duration adverse weather events, events are identified in a second data source, in addition to the Euro4 hindcast dataset (used in Phase 3(a) for event characterisation). This additional data is derived from climate models; hence steps must be taken to validate and calibrate the data where necessary to ensure the characteristics of the data (e.g. the average and variability) are consistent with the equivalent meteorological variables in the observed record. For example, to ensure that the climate model derived data is not biased to being too windy on average. This section firstly introduces the additional source of data in more detail. The methods developed for validating and calibrating this data are then presented and discussed. Following this, adverse weather events identified within all data sources, characterised for regions in Great Britain in different time windows (1-, 3-, 6-, 12- and 24- hours), are explored and discussed. A statistical EVA is then carried out to quantify the return period of events (e.g. 1 in 10 year event) at different climate warming levels (current day, 1.5°C, 2°C, 3°C and 4°C above pre-industrial levels), and an approach for using this quantification to select relevant events from the final dataset is presented.

3.1 Data source

3.1.1 UK Climate Projections 2018 (UKCP18)

The United Kingdom Climate Projections (UKCP18) provide the most recent assessment of how the climate may change in the future (Lowe et al., 2018). They are based on the latest peer-reviewed climate science, inclusive of model data from both the Met Office Hadley Centre

and other international climate-modelling centres. There are 28 global climate model (GCM) simulations providing worldwide coverage at a 60km horizontal resolution for the historical and future periods from 1900-2100. They are separated into two ensembles as they sample uncertainty in different ways:

1. The perturbed physics ensemble (PPE) is made up of 15 variants of the Met Office Hadley Centre model (hereafter referred to as PPE-15). The PPE-15 is created by perturbing a set of parameters within a single land/ocean model to sample a broad range of future outcomes in a systematic way.
2. The Coupled Model Intercomparison Project (CMIP) ensemble is made up of 13 models, produced by 13 separate institutions, from CMIP Phase 5 (hereafter referred to as CMIP-13). Since the models are created independently there is more scope to sample different sources of uncertainty.

The PPE-15 ensemble allows for a quantification of uncertainty owing to parameter uncertainties (how fast ice falls in clouds, for example), while the CMIP-13 ensemble allows for a quantification of uncertainties owing to structural model choices (the type of land and ocean models used, for example).

Wind is a highly variable element whose magnitude can change dramatically depending on local climatology and terrain (Watson, 2014). Burton et al. (2011) explains how these local variations in topology and climatology lead to turbulence, defined as fluctuations in wind speed on a relatively fast time scale. Therefore, capturing local variations in wind speeds is important when characterising ramping stress events. To better capture the smaller scale meteorological conditions relevant for such energy ramping events, this phase of the project utilises the UKCP18 Local projections, which have a significantly higher spatial resolution of 2.2km and provide data at an hourly temporal resolution, compared to Global projections used in Phase 2 (60km spatial and daily temporal resolution). These projections are downscaled from 12 of the PPE-15 but use convection-permitting climate models (hereafter referred to as CPM), which are high resolution models capable of simulating small scale behaviour seen in the atmosphere (as opposed to parameterising it) as well as the influences of mountains, coastlines and urban areas (Kendon et al. 2021).

Each of the 12 projections represents a plausible realisation of the future climate but do sample a narrower uncertainty range compared to the global projections, as they are only downscaled from the Met Office Hadley Centre PPE-15, and not CMIP models (Kendon et al. 2021). Whilst it is worth noting the Local 2.2km projections samples outcomes with a relatively high rate of global warming (i.e., it is known the PPE-15 models run warmer in comparison to

the CMIP models), the methodology used in this phase does not include a calculation of temperature driven demand as in Phase 2, so this is not expected to be of significant impact to the results.

The UKCP18 Local 2.2km projections are available for three twenty-year time slices. The first time period is modelled data for the historical period 1981-2000 i.e., what the climate model ‘projects’ to have happened over this time, as opposed to observations. This data will be used in a similar way to the DePreSys Hindcast data in Phase 2 – to provide additional model years of plausible weather that could have occurred and to sample potentially more extreme weather than was observed in the historical period. Using the historical period from the UKCP18 Local 2.2km projections provides 12 realisations of the 20-year historical period, giving an additional 240 model years. The second and third time slices are projections representing 2021-2040 and 2061-2080 and will be used to capture how events may change in future climates.

3.2 Data calibration

As the UKCP18 datasets are derived from climate models, which are imperfect representations of the physical climate system, the data is likely to contain biases when compared to observations, for example conditions may be generally too windy. As wind capacity factor is calculated from wind speed data using a non-linear wind power curve, any biases in the wind speed data will be greatly amplified by the power curve. For this reason, the UKCP18 10m wind speed data is bias corrected prior to identifying the adverse weather events. Figure 2 below shows spatial maps of the bias in the monthly means of the first ensemble member of UKCP18 data compared to the monthly means of the Euro4 10m wind speed data, where a positive bias means that the wind speed in UKCP18 is on average faster than in Euro4.

Bias between UKCP and Euro4 monthly means (Ensemble 01)

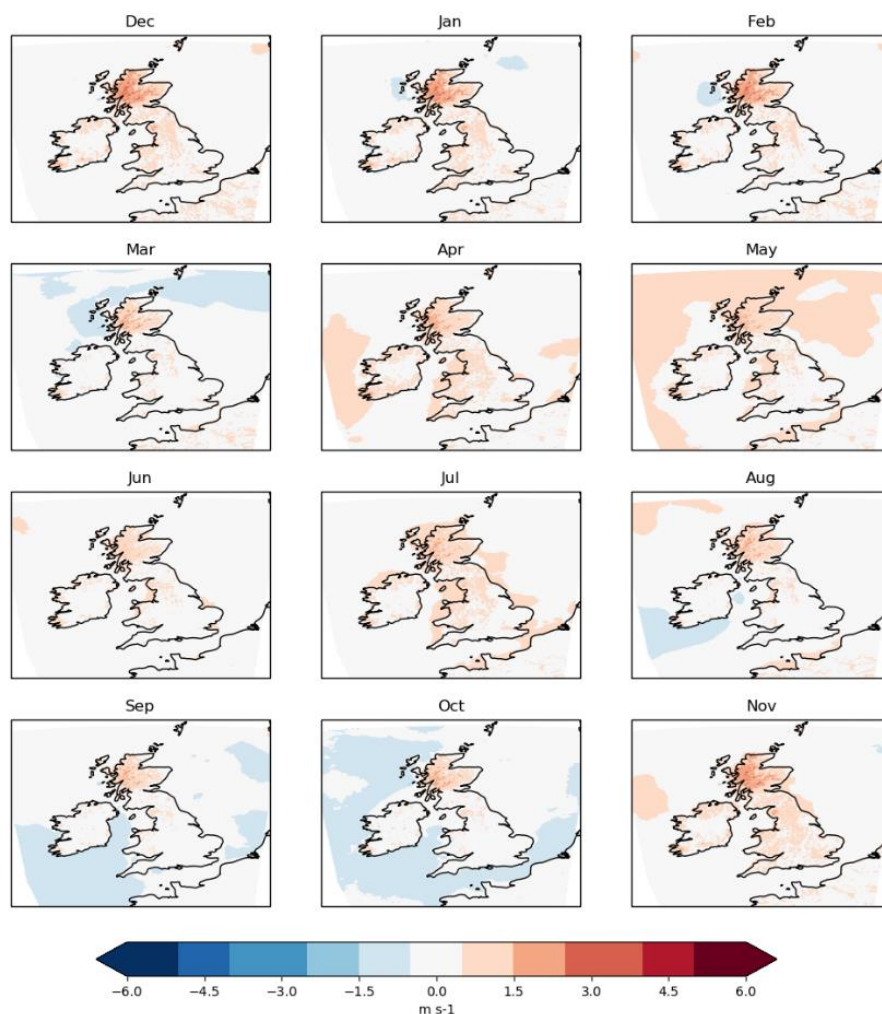


Figure 2: Monthly bias in the mean 10m wind speed of UKCP18 local ensemble member one compared to Euro4 10m wind speed data.

3.2.1 Bias correction of 10m wind speed

The bias correction method applied in Phase 2 was a univariate method, meaning that it is applied to each grid cell and variable separately. This makes the assumption that the temporal, spatial and inter-variable dependence in the data is physically consistent and hence does not need to be corrected. This assumption is thought to be reasonable because the data is derived from a physical climate model. Multivariate bias correction methods allow for multiple variables and locations to be biased corrected together, also allowing any biases in these dependences to be corrected. However, the application of such methods to large climate and weather datasets (such as these) is known to be computationally challenging and cause over-fitting (Cannon, 2018), and hence applying such methods was found to be beyond the scope of this study. Validation work in Section 4.2.1 of Dawkins et al. (2021) showed that applying a

univariate bias correction to UKCP18 Global projections did not cause any unusual dependence structures within the resulting data and achieved consistencies with the mean and standard deviation of the truth data.

The same variance scaling method was used to bias correct the 10m wind speed data from the UKCP18 Local projections. That is, 10m wind speeds from the Euro4 hindcast were used as the truth, and the correction determined from the differences in the mean and standard deviation of each grid cell of Euro4 and UKCP18 during the overlapped period of the two datasets, 1980-2000. Numerical and graphical validation confirmed that this process set the monthly mean and standard deviation of the wind speed in each grid cell of the bias corrected UKCP18 data in the historical time slice to be equal to those of the Euro4 'truth' data

3.2.2 Representing 100m wind speed

Wind capacity factor calculations require turbine height wind speeds, generally around 100m above ground. The wind speed data available in UKCP18 is 10m above the ground, so a method must be utilised to scale this wind speed data to the 100m above ground height. Existing methods such as the log law³ and power law⁴ can be used to scale wind speed from one height to another, however these make assumptions about the surface roughness or wind shear exponent.

An alternative approach, commonly used to correct and adjust wind data (e.g. Dunstan et al. 2016), is to employ a data science modelling technique to represent the relationship between the two wind speed heights (here 10m and 100m) within a dataset that contains both levels (e.g. Euro4), and then use this relationship to scale the data within another dataset that just contains one level (here UKCP18). In this case, and similar to Phase 2, a data science method known as Generalised Additive Modelling (GAM)⁵ is used. This type of model aims to represent a response/target variable (here 100m wind speed) using a combination of smooth functions of other variables (e.g. 10m wind speed).

The relationships between the response variable and other explanatory variables were explored below for a selection of grid cells in the overlapping Euro4 and UKCP18 local domains. These relationships are known to vary depending on surface roughness and orography hence GAMs are fitted separately for each grid cell; data exploration and later, additional model validation, are shown for a selection of these as the spatial resolution of the data is too great to perform for every cell.

³ http://www.met.reading.ac.uk/~marc/it/wind/interp/log_prof/ (Accessed: 14th December 2021)

⁴ <https://websites.pmc.ucsc.edu/~jnoble/wind/extrap/> (Accessed: 14th December 2021)

⁵ <https://datascienceplus.com/generalized-additive-models/> (Accessed: 14th December 2021)

The grid cells chosen are shown below in Figure 3. The selection contains 12 locations across GB and relevant offshore areas.

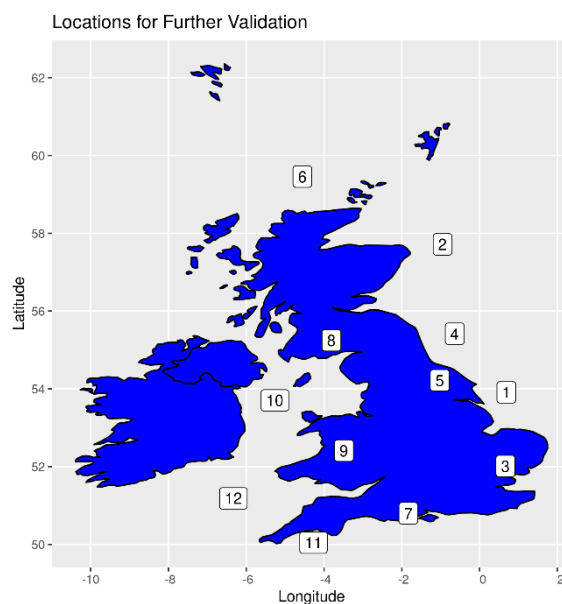


Figure 3: Selected grid cell locations across Great Britain and the surrounding offshore region, labelled from one to twelve.

Figure 4 shows the relationship between daily mean 10m and 100m above ground wind speed, taken from the Euro4 dataset, for a single 4×4 km grid cell, located at location one in Figure 3.

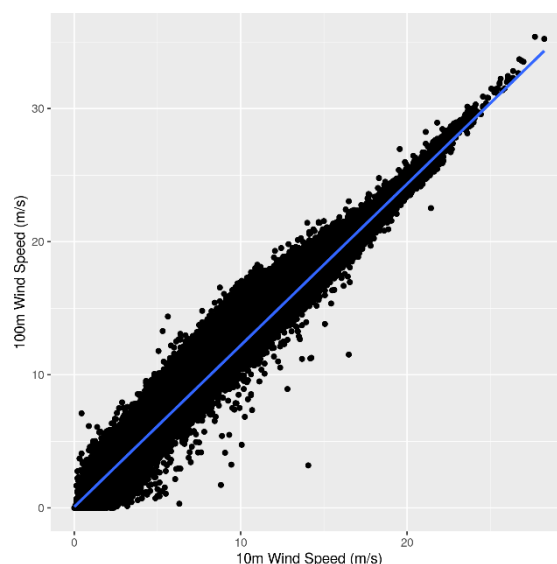


Figure 4: Scatterplot of black points showing 100m above ground wind speed against 10m above ground wind speed in Euro4, at location 1 of Figure 3. The blue line shows the straight line of best fit to these points.

This figure shows how there is a strong linear relationship between 10m and 100m wind speed, with points distributed around the linear regression line of best fit. However, there is

still scatter either side of this line, particularly for 10m wind speeds below 15 m/s, indicating that other factors may be needed to capture the full variability of 100m wind speeds. The relationships between temporal variables (time of year and time of day) and 100m wind speed at the selected locations are also explored.

Through assessing similar plots (not shown), it was found that both the average (median) and the magnitude of the most extreme 100m wind speeds also vary with month of the year. Hence it is expected that there will be value in including time of year in the models. Although less noticeable than the seasonal differences, it also appears that there is a small difference in the distribution of 100m wind speeds depending on the time of day. This suggests that the influence of time of day on 100m wind speed should initially be included in the model and removed if this effect is found not to be statistically significant.

To capture these observed relationships, the GAM is structured such that the response/target variable (100m wind speed) is estimated based on 10m wind speed (which has been bias corrected, see Section 3.2.1), 'month of the year' ('day of the year' cannot be used because UKCP18 uses a 360-day calendar and therefore the 'day of the year' would be inconsistent with Euro4), and 'hour of the day'.

Figure 5 presents an example of the GAM, trained on the Euro4 data in a single grid cell. The three plots show the smooth function fitted to each of the explanatory variables (10m wind speed, month of the year, and time of day).

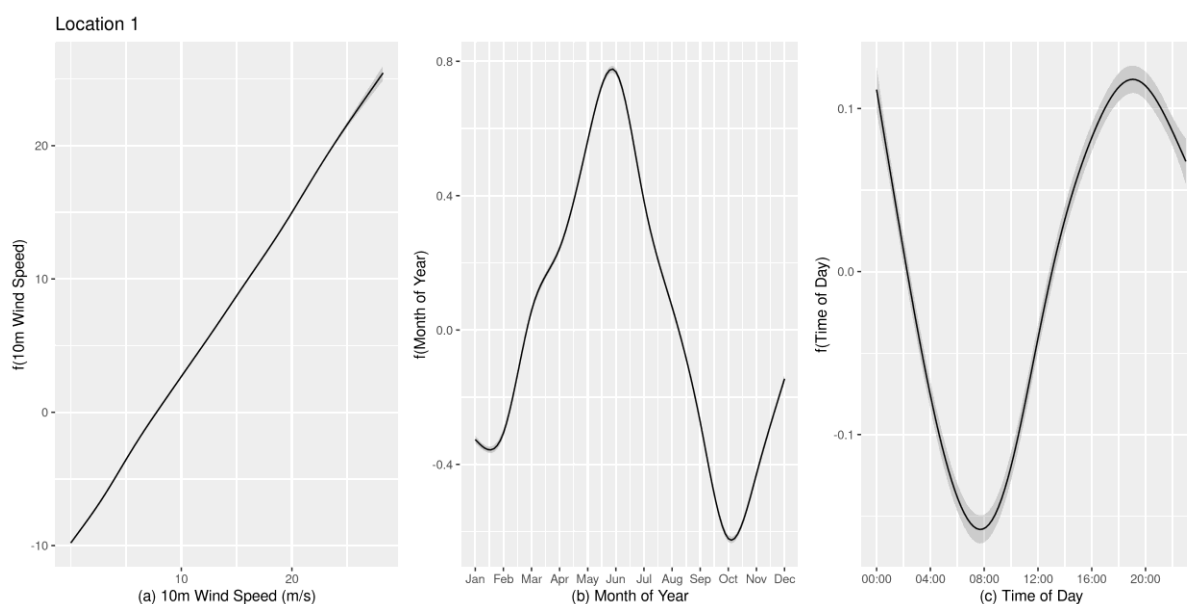


Figure 5: The smooth function fitted by the GAM at location one to (a) 10m wind speed, (b) month of year and (c) time of day to estimate the effect that each has on 100m wind speed when the other two remain constant.

Figure 5 shows how, as well as the strong positive relationship between 10m and 100m wind speed seen in Figure 4, there is a non-linear relationship with the month of the year (100m wind speed is generally higher between March and September, considered where the other explanatory variables are fixed). There is also a small but statistically significant effect (with a p-value of less than 0.001, as with the other two explanatory variables) due to the time of day –for a fixed 10m wind speed and month of the year, the time of day is expected to influence the 100m wind speed by up to 0.2m/s. Similar relationships are found in other grid cells and can be seen in other test locations in the appendix.

The three smooth functions fitted can be used to predict 100m wind speed based on the three explanatory variables, by summing $f(\text{variable})$, where the value of the variable is representative of that given hour (i.e. the 10m wind speed, month of year, hour of the day). A cross-validation method is used to validate the models. The GAM is trained on a subset of the Euro4 data (80%), and then used to estimate 100m wind speed for the remaining 20% of the (un-modelled) test data. An example of the relationship between the predicted and true 100m wind speed in one grid cell is presented in Figure 6. The GAM is found to provide a high level of predictability, as shown in Figure 6, in which 96% of the variance in the Euro4 100m wind speed data is explained by the GAM model, with 100% equating to perfect predictability. The GAM appears to be performing equally well when assessed with the test (unseen) subset of the data.

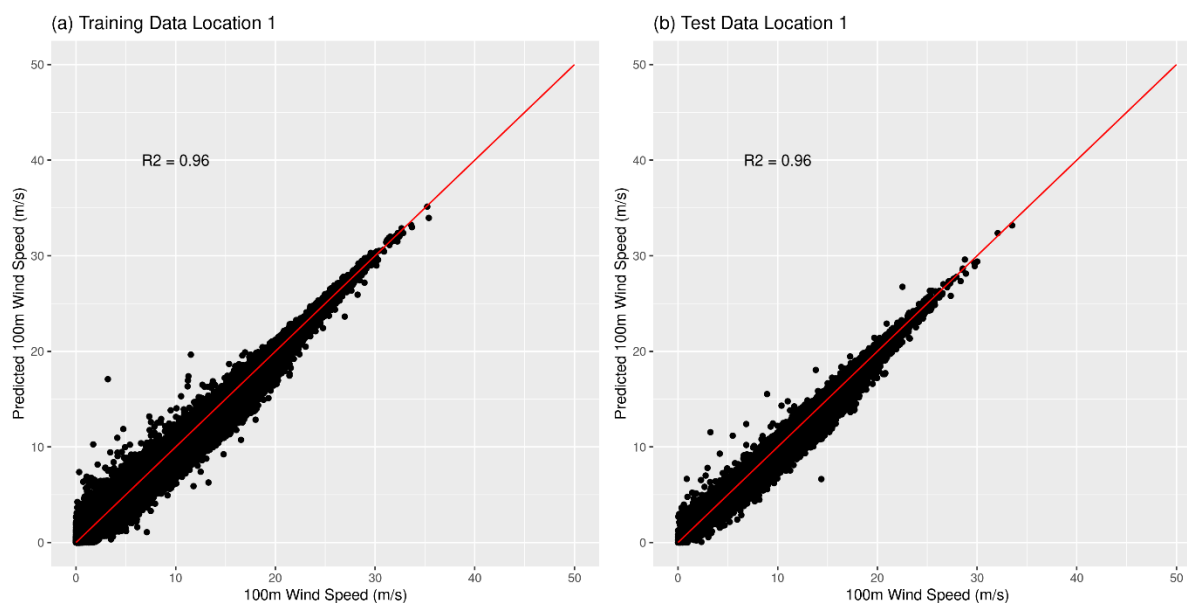


Figure 6: Scatterplots of predicted Euro4 100m wind speed against true Euro4 100m wind speed at location one, (a) for the training subset of the data and (b) for the test subset of the data. The $y=x$ line (where the prediction is equal to the truth) is shown in red.

Similarly performing models are fitted to each grid cell of the UK onshore and offshore regions. Figure 7 shows a spatial map of the R^2 (proportion of variation in the Euro4 100m wind speed data) explained by the model in each grid cell that a model is fitted to, for the training data and the test data.

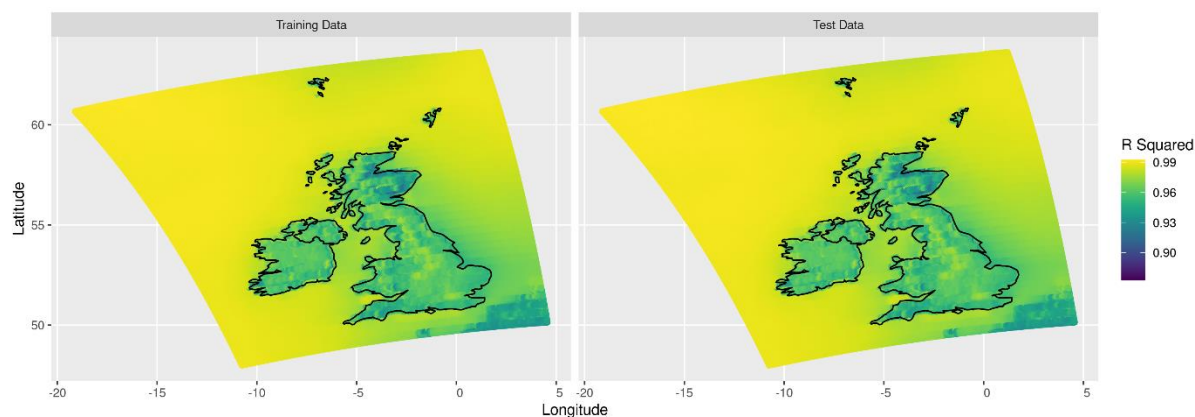


Figure 7: (a) R^2 of the GAM fitted to each grid cell, applied to the training subset of Euro4 100m wind speed data and (b) R^2 of the GAM fitted to each grid cell, applied to the test subset of Euro4 100m wind speed data.

Figure 7 confirms that the GAMs have a similar level of accuracy across the GB and offshore domain as they do in the 12 grid cells selected for additional validation, with at least 87% of variation in the 100m wind speed data explained by the model in every grid cell, even when applied to unseen data that was not used to fit the model.

These GAMs are applied to the bias corrected, 10m wind speed data from the 12 UKCP18 Local projections over the three time slices (1981-2000, 2021-2040 and 2061-2080). This estimated 100m wind speed data was further validated to confirm that the characteristics of this estimated UKCP18 100m wind speed data are consistent with the 100m wind speeds in the Euro4 record. Hence, it can be used to estimate wind capacity factors within this study.

3.3 Exploring adverse weather scenarios in Euro4 and UKCP18

The methods described in Section 2 (and detailed further in Dawkins and Rushby, 2021 and Pearce et al., 2021) are applied to the two data sources: Euro4 hindcast (1979-2014) and the calibrated UKCP18 Local projections (1981-2000, 2021-2040 and 2061-2080). In this section we present the analysis of wind ramping events identified in the Euro4 and UKCP18 data.

Initially the frequency of different magnitude ramping events is compared for the overlapping period of the Euro4 hindcast and UKCP18 historical time slice (1981-2000), with each of the twelve members of the UKCP18 ensemble displayed separately.

Figure 8, equivalent to Figure 8(c) and (f) in Cannon et al. (2015) shows, for each time window (one per row) and data source (coloured lines), the number of times in an average year (y-

axis) that a ramp event is observed reaching or exceeding a threshold of ΔCF (x-axis), for the defined Offshore North region. The right-hand panel presents an exploration of the less frequent ramping events for each time window i.e., focusing on events reaching a threshold change less than 150 times (number of hours) in an average year. Similar plots can be seen for the other four defined regions in Appendix 1-4.

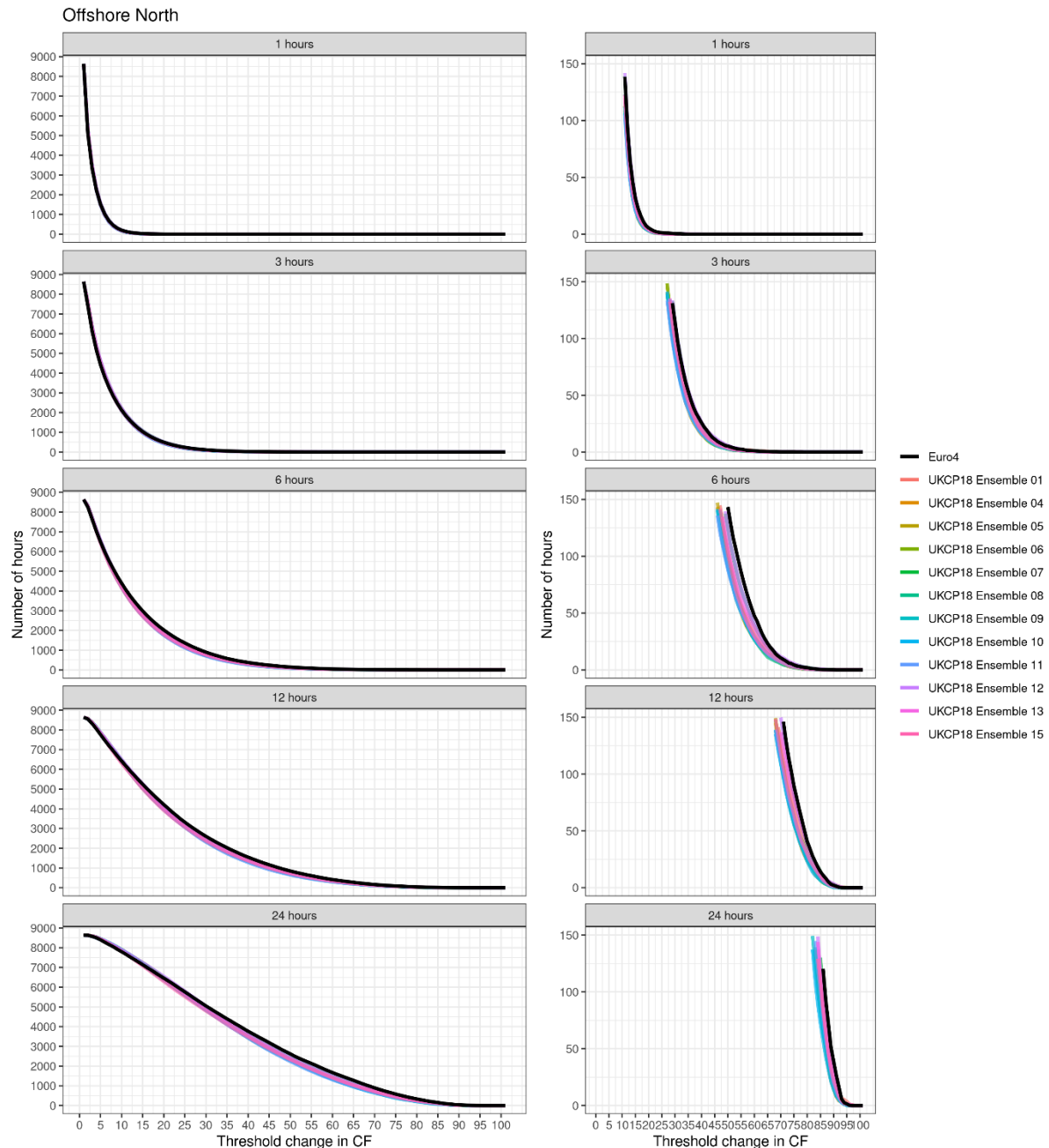


Figure 8: The number of hours in an average year (y-axis) that a ramp event is observed reaching or exceeding a threshold of ΔCF (x-axis), for the Offshore North region. The black lines represent the Euro4 data and each of the other coloured lines on the plot represent a different UKCP18 ensemble member with a row per time window (1-, 3-, 6-, 12- and 24- hour time windows) identified in the top grey bar. The right-hand panel presents an exploration of the less frequent ramping events for each time window i.e., focusing on events reaching a threshold change less than 150 times (number of hours) in an average year between 1981 and 2000.

Changes in capacity factor above each threshold are seen for a similar number of hours per year in the Euro4 and UKCP18 records, particularly in shorter time windows. In both records, larger changes in capacity factor occur less frequently as the definition of these events is more stringent, and similarly more extreme events are seen less often in shorter time windows. In longer time windows, particularly the 6-hour window, there is a wider range of frequencies across the UKCP18 ensemble members for each threshold change, and the more extreme ramping events are seen for a larger number of hours per year in Euro4 than in UKCP18. In a 1-hour window, a change in capacity factor exceeding 20 is seen on average 5.5 times a year in Euro4 whereas in UKCP18 this ranges between 2.9 and 5.3. In the 6-hour window, the same change in capacity factor is exceeded on average 2025 times a year in Euro4 and between 1755 and 1921 times in UKCP18. In a 24-hour window, a change in capacity factor exceeding 80 occurs 335 times a year on average in Euro4, or between 199 and 293 times in UKCP18. However, broadly there is very strong agreement between Euro4 and UKCP18 in terms of ramping frequency. This provides confidence that the UKCP18 dataset is able to reproduce short-term wind fluctuations as required to provide insights on ramping events. Nonetheless, in the statistical extreme value analysis (Section 3.4), a climate model bias term is included to adjust for any differences in ramping events between two data sources.

In addition to providing an extra 240 years of plausible ramping events which could have happened in the past but did not, the ramping events identified in the future time slices of the UKCP18 local projections are also be used to assess changes in ramping events due to climate change. Figure 9 shows the number of hours (x-axis) in each year (y axis) that the change in capacity factor in the Offshore North region exceeds 20, in both Euro4 and UKCP18. Each row (and colour) represents a different time window (1-, 3-, 6-, 12- and 24- hour time windows) and the years are grouped into three columns, with the left showing the historical period (Euro4 and historical UKCP18 time slice), the middle showing the first future time slice of UKCP18, and the right showing the later future time slice of UKCP18. The number of hours per year the threshold is exceeded in Euro4 are marked with black crosses, and the spread of the number of hours per year that the threshold is exceeded in each ensemble member of UKCP18 are shown by a boxplot for each year. For consistency across years, the first and

last calendar year of each UKCP18 time slice are not included in this figure as they do not contain a full year of data.

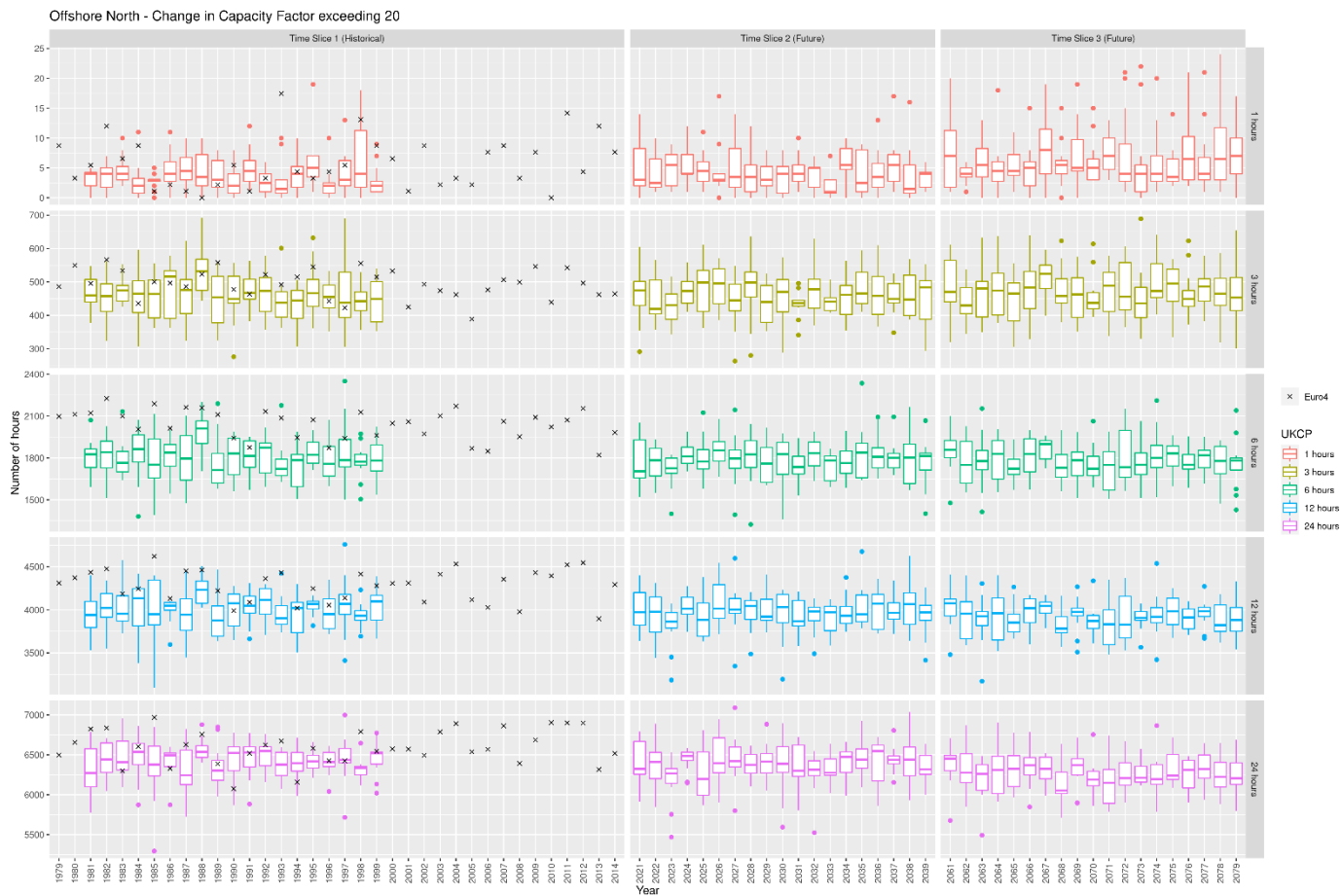


Figure 9: The number of hours (x-axis) in each year (y axis) that the change in capacity factor in the Offshore North region exceeds 20, in both Euro4 and UKCP18. Each row (and colour) represents a different time window (1-, 3-, 6-, 12- and 24- hour time windows) and the years are grouped into three columns, with the left showing the historical period (Euro4 and historical UKCP18 time slice), the middle showing the first future time slice of UKCP18, and the right showing the later future time slice of UKCP18. The number of hours per year the threshold is exceeded in Euro4 are marked with black crosses, and the spread of the number of hours per year that the threshold is exceeded in each ensemble member of UKCP18 are shown by a boxplot for each year.

For the historical period, UKCP18 shows more variation in the number of times the threshold of 20 is exceeded in a year, which shows the value of this dataset in providing plausible events which may not have been sampled in the historical record. This is shown by this magnitude of ramping event occurring in a 3-hour window between 276 and 692 times per year in UKCP18 compared to 389 to 566 times in Euro4.

When interpreting figures such as this, it is important to note that climate models produce a projection - not a forecast - of what may happen in the future, and it is not possible to conclude the number of hours that a change in capacity factor will exceed 20 in a specific year in the future. However, by considering the years and ensemble members for each time slice of

UKCP18 as a whole, there may be an indication of a signal for how often these ramping events may occur in the future.

In this case the frequency of ramping events exceeding a change in capacity factor of 20 (in the Offshore North region) there appears to be a slight tendency for an increase in ramping frequency: In the final time slice for the 1-hour window there are 13 years in UKCP18 that exceed the maximum ramping frequency observed in Euro4 for the historical period (seen in 1993). The UKCP18 only exceeds this Euro4 frequency once in the historical period

However the future period ramping frequency is in general very similar to the historical time slice of UKCP18 and Euro4.

Figure 10 shows similar to Figure 9, but now displaying the frequency of a higher threshold, a change in capacity factor of 80, is exceeded in the Offshore North region, in Euro4 and UKCP18.

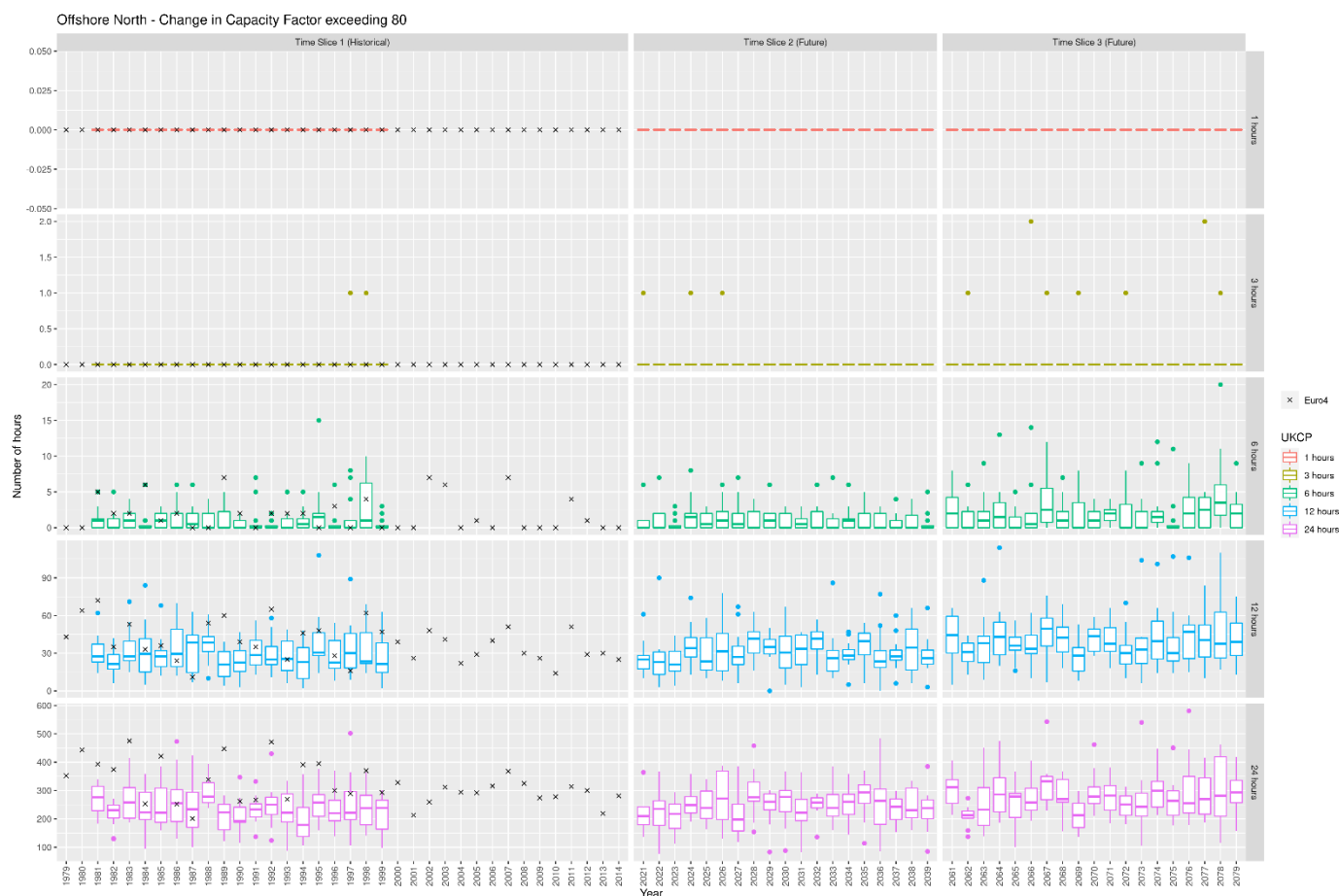


Figure 10: The number of hours (x-axis) in each year (y axis) that the change in capacity factor in the Offshore North region exceeds 80, in both Euro4 and UKCP18. Each row (and colour) represents a different time window (1-, 3-, 6-, 12- and 24- hour time windows) and the years are grouped into three columns, with the left showing the historical period (Euro4 and historical UKCP18 time slice), the middle showing the first future time slice of UKCP18, and the right showing the later future time slice of UKCP18. The number of hours per year the threshold is exceeded in Euro4 are marked with black crosses, and the spread of the number of hours per year that the threshold is exceeded in each ensemble member of UKCP18 are shown by a boxplot for each year.

A change in capacity factor of 80 is never seen in UKCP18 or Euro4 during a 1-hour window. In the 3-hour window a ramping event of this size was never seen in Euro4, however it is seen at most once a year in the historical UKCP18 dataset. This is an indication that the UKCP18 dataset is doing well at representing plausible extreme scenarios that did not happen in the historical record. In the future (between 2061 and 2079) this is seen at most twice a year. In the longer time windows the maximum number of hours that change of 80 is seen in a year is in general slightly greater in later future time slice compared to historical or first future time slices of UKCP18 (for the 6-hour window, at most 20 times compared to 15). This change has not been assessed for statistical significance; this assessment is undertaken using the EVA methods. Non-stationary (accounting for changes in time based on global mean surface temperature), statistical extreme value analysis, as used by (Dawkins et al., 2021b) is an appropriate method to identify if specific change in capacity factors occur significantly more or less often at various future warming levels.

Similar results were found for the other four defined regions (not shown here).

3.4 Statistical extreme value analysis to quantify adverse weather in different climates

The aim of this study is to produce a dataset of adverse weather scenarios, characteristic of various extreme levels (i.e. return periods), and climate change warming levels. Specifically, the 1 in 2, 5, 10, 20, 50 and 100 year return period events for warming levels representative of current day (global mean temperature 1.2°C above pre-industrial temperature) and - if distinct from current day – global mean temperature 1.5°C, 2°C, 3°C, and 4°C above pre-industrial temperature, are to be shared (Butcher and Dawkins, 2020).

To achieve this, a non-stationary statistical EVA⁶ is implemented (Coles, 2001), based on the magnitude (maximum change in capacity factor across a region in a fixed period of time) of adverse weather scenarios identified in the two data sources (as presented in Section 3.3). This analysis provides a return level curve for each defined region (Offshore North, Offshore South, Onshore North, Onshore East and Onshore West), length of time window (1-hour, 3-hour, 6-hour, 12-hour and 24-hour) and global warming level of interest (1.2, 1.5, 2, 3, 4°C above pre-industrial). This analysis can then be used to identify the extremity of an adverse weather scenario expected to occur on average once every N years (i.e. a 1 in N year event) for that given region, time window and global warming level.

As described in Section 5.3 and Figure 64 of Dawkins (2019), and implemented in (Dawkins et al., 2021b), a statistical extreme value distribution, such as the Generalised Pareto Distribution (GPD)⁷, can be fitted to the extremes of a variable (e.g. temperature above a high threshold), and used to parametrically estimate the probability of observing a value of a given magnitude (e.g. the probability of observing a temperature of 30°C). That is, the parameters that explain the shape of the fitted GPD (the scale and shape parameters⁷) can be used within the GPD probability density function⁷ to calculate this event probability. This probability can then be equated to a return period (or recurrence interval), representative of the number of years on average you would have to wait to see an event of the same magnitude. For example if the fitted GPD specifies a 0.01 (or 1%) probability of observing a temperature of 30°C in a year, then this event has been modelled as occurring on average once every 100 years, equivalent to having a return period of 100 years. Note that these values are purely for demonstration and are not based on real data.

⁶ A glossary of acronyms is presented in Section 7

⁷ <http://www.nematrian.com/GeneralisedParetoDistribution> (Accessed 28/05/2021)

Further, it may be expected that this probability will change over time, for example due to climate change. This means that the modelled variable (e.g. temperature) is expected to be non-stationary, and hence a non-stationary (changing over time) GPD should be fitted instead. In this case, the parameters of the GPD, and in some cases the GPD high threshold (Brown et al., 2014), are able to vary in time by conditioning on a relevant explanatory variable such as global mean surface temperature (GMST), known to be a good representation of the magnitude of climate change (Brown et al., 2014). In the non-stationary case, the parameters of the GPD depend on the relevant explanatory variable (e.g. GMST) and hence the GPD takes on a different shape for any given value of this variable. For example, this could mean that the fitted GPD specifies a 0.01 (or 1%) probability of observing a temperature of 30°C in any given year for the current day global warming level (1.2°C above pre-industrial), but a 0.05 (or 5%) probability of observing a temperature of 30°C in any given year for a warming level of 2°C above pre-industrial. This means that this is a 1 in 100 year event in the current day climate, but a 1 in 20 year event (occurring on average 5 times in 100 years) in the warmer climate. As above, these values are purely for demonstration and are not based on real data.

This non-stationary EVA approach has previously been used by Brown et al. (2014) (as discussed in Section 5.2.5 of Butcher and Dawkins (2020)), to produce time-dependent projections of future extreme rainfall and temperature in the UK. Additionally it has been applied by (Dawkins et al., 2021b) to the duration and severity of long-duration adverse weather scenarios. Similar to the above example, Brown et al. (2014) and (Dawkins et al., 2021b) condition their EVA model parameters on GMST, allowing for extremes to be estimated for any given warming level of interest. In addition, the model is fitted to both climate projections, so future warming levels can be considered, as well as historical observations within an overlapping time period, to allow for the climate projections to be bias corrected. This bias correction is achieved by conditioning the EVA model parameters on a bias term (as well as global mean temperature) that is only applied to data from the climate projections. This term can then be 'turned off' to allow for non-biased estimates of future extremes (see Brown et al. (2014) for more detail).

In this study, a similar approach is used to quantify the extremes of the adverse weather event magnitudes. This allows for the return period of the magnitude to be quantified, and subsequently used to pick relevant events for the final dataset. For example, allowing for insights such as: a 3-hour ramping event in the Offshore North region expected to occur on average once every 20 years (1 in 20 year event) in the current day climate (warming level 1.2°C above pre-industrial) has a maximum change in capacity factor of 68.1. Similar to Brown et al. (2014) and (Dawkins et al., 2021b), here, a non-stationary EVA model is fitted to ramping

event magnitudes (the maximum change in capacity factor in a given time window and region) taken from both climate projections and historical data, and the parameters of the EVA model (here a GPD) are conditioned on GMST and a climate model bias term. Brown et al. (2014) fit their EVA model to each climate model projection individually to allow for the climate model structural and parametric uncertainty to be fully captured. Here, however, as in (Dawkins et al., 2021b) since adverse weather events rather than raw meteorological data are being modelled, the relatively small sample size of events in an individual climate projection result in the fitted EVA model being very sensitive to outliers (extreme high or low values) in the UKCP18 data. Hence here the UKCP18 adverse weather events, for the whole PPE ensemble, are pooled together into one EVA model for each event type and metric. In addition, in this study, the UKCP18 local projections – the twelve downscaled ensemble members of the Hadley Centre PPE-15 - are used. This means climate model structural uncertainty is not captured here. The Hadley Centre models are known to become warmer more rapidly than the CMIP5 models over the future period (Figure 5.2 of Murphy, J. M. et al. 2018). This is, however, not an issue within this analysis because the extremity of events is captured in terms of warming level, not time.

As well as including historical *observed* events (from Euro4), here, the UKCP18 historical time slice events are also included within each EVA model. These UKCP18 events, taken from 240 years of meteorological data, are treated as additional historical observations similarly to the use of DePreSys⁸ in (Dawkins et al., 2021b), thought to be acceptable based on the numerous validations presented in this report. This therefore greatly reduces the uncertainty in the high return period estimates. That is, since the UKCP18 historical events represent well over 100 years of meteorological information, estimating the 1 in 100 year return period event can be done with much greater certainty than if only events from the 36 Euro4 years of data were used.

As described in Section 3.3, Section 3.4 and Figure 3 of (Pearce et al., 2021), the maximum change in capacity factor could occur at any point during a given time window, and therefore where two-time windows may overlap, there is the potential for repeated data points where one ramping event is double counted, and hence the events being temporally correlated. This can lead to a misrepresentation of the return period of events (Coles, 2001). In the empirical EVA of (Pearce et al., 2021) this is accounted for using de-clustering. In this statistical extreme value analysis, the de-clustering is achieved through the inclusion of an extremal index (Coles,

⁸<https://www.metoffice.gov.uk/research/approach/modelling-systems/unified-model/climate-models/depresys> (Accessed 01/06/2021)

2001), a parameter of the GPD which measures the degree of clustering in the extremes of events (Smith and Weissman, 1994).

As the change in capacity factor is defined for values between 0 (no change) and 100 (from zero generation to full generation or the reverse), the magnitude of events to be modelled must be bounded between 0 and 100. A GPD is a continuous distribution, and so the magnitudes of the ramping events must be transformed to a continuous domain before they can be modelled. The logit transformation⁹ is applied to the magnitude of the change in capacity factor for each ramping event, and the GPD is fitted to the transformed values instead. Once the model has been fitted, the inverse of the logit transformation is applied to the return level curve, meaning that the return levels estimated from the parameters are bounded between 0 and 100 without invalidating the assumptions needed for this type of modelling.

When implementing a GPD EVA analysis, a suitable high threshold of the modelled variable (e.g. transformed event magnitude) must be selected, above which the GPD is fitted. This is done to satisfy the statistical assumptions of the GPD (Coles, 2001), and to ensure the GPD fits well to the extreme values in the data. Here, it is essential that the EVA model is able to represent the (relatively low) 1 in 2 year event level, to allow for this event to be captured within the final dataset, as specified in the scoping phase of the project (Butcher and Dawkins, 2020). De-clustering the adverse weather events with the extremal index means that the sample of events is effectively reduced and so the 1 in 2 year event level identified from the full record would not be the same as a 1 in 2 year event identified following de-clustering. Sensitivity testing was used to determine the appropriate threshold which allowed for modelling of the 1 in 2 year event, and also was appropriately extreme to model well more extreme events. For each of the 25 adverse weather event region and time window combinations to be modelled (i.e. Offshore North 1-hour window, Offshore North 3-hour window, Offshore South 1-hour window, etc.), the percentile of the modelled variable equivalent to the 1 in 0.1 year event is calculated and used as the threshold above which to fit the GPD.

The definition of a ramping event (one occurring every hour) in this work means the median number of each event type, for example 6-hour ramping events in the Offshore North region, occurring per year across Euro4 identified per year is 8760. Hence the percentile of the modelled variable equivalent to the 1 in 0.1 year event is scaled by the number of events per year, which for events occurring in 6, 12, and 24 hour windows is 8760. Due to spurious

⁹ <https://dictionary.apa.org/logits> (Accessed 22/02/2022)

midnight ramps excluded from the analysis of Euro4 ramping events - see (Pearce et al., 2021) there are 8030 1-hour events and 7300 3-hour events per year and so the corresponding number of events per year is used to scale the percentile for each event type. The resulting percentile thresholds used in each GPD model are shown in Table 1. In all cases, these thresholds were found to be high enough to accurately model the observed 1 in 100 year extreme level (the highest level to be selected for the final data set).

Finally, a model selection process was carried out to explore the most appropriate EVA model structure. Non-stationary GPD models were fit to the 6-hour ramping events in the Onshore North region to explore two different model structures:

- (1) Different climate model bias terms for each of the twelve downscaled UKCP18 PPE-15 members
- (2) A single bias term for all twelve of the downscaled UKCP18 PPE-15 members

In both cases the effect of GMST is modelled in the GPD scale parameter and the extremal index (for de-clustering) is also included.

Structure (1) resulted in large uncertainties in the model which would make it difficult to draw conclusions due to the overlap in the return level of a 1 in 50 and 1 in 100 year event for example. This is due to the relatively small sample size of events in an individual climate projection causing the fitted EVA model to be very sensitive to outliers. By treating all ensemble members as one sample, as in (Dawkins et al., 2021b), thus increasing the sample size, the uncertainty in the GPD model fit is reduced. For this reason, model structure (2) is selected for the following analysis.

The EVA model structure (2) is fitted to each adverse weather event type and metric combination. As in (Dawkins et al., 2021b) this is done using a Bayesian statistical modelling framework, using the `extRemes` package¹⁰ in the R statistical computing environment, resulting in an estimated 'posterior' distribution¹¹ of values for each model parameter. These model fits are summarised in Table 1. Note that these parameters correspond to the GPD fitted to transformed data and the inverse transformation is applied to the return level curves constructed from these before interpreting the models.

¹⁰ <https://cran.r-project.org/web/packages/extRemes/extRemes.pdf> (Accessed 11/06/2021)

¹¹ <https://towardsdatascience.com/probability-concepts-explained-bayesian-inference-for-parameter-estimation-90e8930e5348> (Accessed 29/05/2021)

Region	Time Window	GPD threshold percentile	GPD scale intercept term	GPD scale bias term	GPD scale GMST change term	GPD shape parameter	GPD Extremal Index
Offshore North	1-hour	0.99875	-1.5716	-0.0475	0.0420	-0.0606	0.3035
Offshore North	3-hour	0.99863	-1.3503	-0.0654	0.0432	-0.0182	0.2642
Offshore North	6-hour	0.99886	-1.1878	-0.0369	0.0329	-0.0837	0.2640
Offshore North	12-hour	0.99886	-1.4725	0.1043	0.0233	-0.1148	0.2416
Offshore North	24-hour	0.99886	-1.5952	0.0490	-0.0014	-0.0893	0.1488
Offshore South	1-hour	0.99875	-1.3437	-0.1182	0.0395	-0.0173	0.4659
Offshore South	3-hour	0.99863	-1.3400	-0.1128	0.0414	-0.0668	0.3679
Offshore South	6-hour	0.99886	-1.6305	-0.1651	0.0386	0.0189	0.2583
Offshore South	12-hour	0.99886	-1.5083	-0.0836	0.0563	0.0577	0.2221
Offshore South	24-hour	0.99886	-1.5610	0.0872	0.0782	-0.0752	0.1682
Onshore North	1-hour	0.99875	-1.6530	-0.1403	-0.0137	-0.0712	0.5821
Onshore North	3-hour	0.99863	-1.5995	-0.1235	-0.0133	-0.0410	0.4737
Onshore North	6-hour	0.99886	-1.5916	-0.0890	-0.0158	-0.0527	0.3672
Onshore North	12-hour	0.99886	-1.5876	-0.1787	-0.0032	-0.1012	0.2351
Onshore North	24-hour	0.99886	-1.9421	-0.1368	-0.0020	-0.1391	0.1120
Onshore East	1-hour	0.99875	-1.6041	-0.1489	-0.0212	-0.0653	0.7452
Onshore East	3-hour	0.99863	-1.5988	-0.1005	-0.0078	-0.0331	0.5308
Onshore East	6-hour	0.99886	-1.3990	-0.1178	-0.0058	-0.0708	0.4352
Onshore East	12-hour	0.99886	-1.4327	-0.0486	0.0234	-0.1354	0.2256
Onshore East	24-hour	0.99886	-1.6451	-0.0994	-0.0149	-0.2317	0.1369
Onshore West	1-hour	0.99875	-1.6734	-0.1292	0.0019	-0.0720	0.6934
Onshore West	3-hour	0.99863	-1.6321	-0.0945	-0.0027	-0.0330	0.4143
Onshore West	6-hour	0.99886	-1.5682	-0.1159	0.0133	-0.0256	0.3032
Onshore West	12-hour	0.99886	-1.4456	-0.1949	-0.0111	-0.1287	0.2132
Onshore West	24-hour	0.99886	-1.7301	-0.1429	0.0320	-0.2252	0.1053

Table 1: Table summarising the non-stationary GPD fits to each adverse weather event type. The GPD threshold (column 3) is the percentile of the transformed change in capacity factor, above which the GPD is fitted, calculated as the percentile equivalent to a 1 in 0.1 year event. The GPD has two parameters: scale and shape. The scale parameter is modelled as varying over time (non-stationary) conditioned on GMST and a climate model bias term, hence the scale parameter is a combination of an intercept term (column 4), the climate model bias term (column 5) and the GMST change effect (column 6). The shape parameter is modelled as being stationary and unbiased in the climate model (column 7). The extremal index parameter measures the extent of clustering in the event data. For each model parameter, the Bayesian posterior distribution mean is given (i.e. the best estimate of this value from the model).

Smaller extremal index values indicate a larger average cluster size, so from Table 1 we can see that as the length of the time window increases, in general the average cluster size increases, which is to be expected as there is greater overlap between neighbouring windows. The posterior mean of the GPD scale bias and GMST change parameters (which represent the difference between the two data sources and the effect of climate change) show varying directions for each combination region and time window, which is likely to reflect the lack of a conclusive climate change signal in the underlying wind data.

Figure 11 - Figure 15 and Table 2 - Table 26 present the final results of the statistical EVA. The plots indicate that for each event type there is not a material difference in the return level of maximum change in capacity factors across the five warming levels, with many of the return

level curves representing each warming level being indistinguishable from each other. In all cases of the return periods of interest (1 in 2, 5, 10, 20, 50 and 100 years), as shown by the corresponding tables, the return levels at the 1.5, 2, 3, and 4 (°C) warming levels are within or only slightly (up to a change in capacity factor of 0.2) outside of the 95% credible interval of the change in capacity factor expected at the 1.2 (°C) (present day) warming level. For this reason, any event which is identified through this work as representative of the 1.2 (°C) warming level for a given event type and return period, is also deemed to be representative of the 1.5, 2, 3, and 4 (°C). Events for the final dataset will therefore be selected using the 1.2 (°C) warming return levels only.

Table 2 - Table 26 summarise the key return levels of interest within this study, and therefore highlight the extremity of events that should be used to represent each return period and in the final 'Adverse Weather Scenarios for Future Electricity Systems' dataset. For example, it is shown in Table 2 that the 1 in 20 year return level event, over a 1-hour time window and the Offshore North region, in the current day climate (warming level 1.2°C above pre-industrial) has a maximum change in capacity factor of 29.5 – 33. This means that 1-hour, Offshore North events in this range should be selected to represent this event type and return period across all warming levels in the final dataset.

The results of this statistical EVA can also be used to more accurately quantify the extremity of the Euro4 wind ramping events identified and presented in the Phase 3 (a) report (Pearce et al., 2021). For example a 1 in 20 year event in a 3-hour window in the Onshore West region, identified in (Pearce et al., 2021) saw a maximum change in capacity factor of 78.38. Using the statistical EVA developed in this phase of the project, the 1 in 20 year event of this type would be expected to have a maximum change in capacity factor of 54.2. These EVA models, summarised in the curves presented in Figure 11 - Figure 15, can be used in a similar way to estimate the return period of any of the Euro4 events presented in the Phase 3 (a) report (Pearce et al., 2021).

WL (°C)	RL:2 years	RL:5 years	RL:10 years	RL:20 years	RL:50 years	RL:100 years
1.20	22.9 (22.3,23.6)	26.1 (25.2,27.3)	28.5 (27.4,30.1)	31 (29.5,33)	34.3 (32.3,37)	36.7 (34.4,39.9)
1.50	23 (22.4,23.7)	26.2 (25.3,27.4)	28.7 (27.5,30.3)	31.2 (29.7,33.3)	34.5 (32.6,37.3)	37 (34.6,40.3)
2.00	23.1 (22.5,23.9)	26.4 (25.5,27.7)	29 (27.7,30.7)	31.6 (30,33.7)	35 (33,37.9)	37.5 (35.1,41)
3.00	23.4 (22.8,24.3)	26.9 (25.8,28.4)	29.6 (28.2,31.6)	32.3 (30.6,34.8)	35.9 (33.7,39.2)	38.6 (36,42.6)
4.00	23.7 (23,24.7)	27.4 (26.2,29)	30.2 (28.6,32.4)	33.1 (31,35.9)	36.9 (34.3,40.6)	39.8 (36.7,44.1)

Table 2: Table summarising the 1 in 2, 5, 10, 20, 50, and 100 year return level (RL) of the maximum change in capacity factor in a 1 hour window and the Offshore North region for each warming level (WL) of interest. In each case, the Bayesian posterior mean (best estimate) is given, with the 95% credible interval around this shown in brackets. These values summarise the curve shown in Figure 11 (a).

WL (°C)	RL:2 years	RL:5 years	RL:10 years	RL:20 years	RL:50 years	RL:100 years
1.20	54.3 (53.1,55.5)	60 (58.3,61.8)	64.2 (62,66.4)	68.1 (65.6,70.7)	72.8 (70,75.7)	76 (73,79.1)
1.50	54.4 (53.2,55.6)	60.2 (58.4,62.1)	64.4 (62.2,66.6)	68.3 (65.8,70.9)	73.1 (70.2,76.1)	76.3 (73.2,79.5)
2.00	54.6 (53.4,55.9)	60.6 (58.7,62.4)	64.8 (62.6,67.1)	68.8 (66.2,71.4)	73.6 (70.7,76.6)	76.9 (73.7,80)
3.00	55.1 (53.8,56.4)	61.3 (59.3,63.2)	65.7 (63.3,68)	69.8 (67,72.5)	74.7 (71.5,77.7)	78 (74.6,81.2)
4.00	55.7 (54.2,57.1)	62.1 (59.9,64.2)	66.6 (64,69.2)	70.9 (67.9,73.7)	75.8 (72.5,79)	79.2 (75.5,82.5)

Table 3: Table summarising the 1 in 2, 5, 10, 20, 50, and 100 year return level (RL) of the maximum change in capacity factor in a 3 hour window and the Offshore North region for each warming level (WL) of interest. In each case, the Bayesian posterior mean (best estimate) is given, with the 95% credible interval around this shown in brackets. These values summarise the curve shown in Figure 11 (b).

WL (°C)	RL:2 years	RL:5 years	RL:10 years	RL:20 years	RL:50 years	RL:100 years
1.20	78.6 (78,79.4)	82.4 (81.5,83.3)	84.7 (83.8,85.8)	86.7 (85.6,87.8)	88.8 (87.7,90)	90.1 (89,91.3)
1.50	78.7 (78.1,79.5)	82.5 (81.6,83.4)	84.8 (83.8,85.9)	86.8 (85.7,87.9)	88.9 (87.8,90.1)	90.2 (89.1,91.4)
2.00	78.8 (78.2,79.6)	82.6 (81.8,83.6)	85 (84,86.1)	87 (85.9,88.1)	89.1 (88,90.3)	90.4 (89.2,91.7)
3.00	79.1 (78.4,80)	83 (82,84.1)	85.4 (84.3,86.6)	87.4 (86.2,88.6)	89.5 (88.3,90.8)	90.8 (89.5,92.1)
4.00	79.4 (78.6,80.4)	83.4 (82.3,84.6)	85.8 (84.6,87.1)	87.8 (86.5,89.1)	89.9 (88.6,91.3)	91.2 (89.8,92.5)

Table 4: Table summarising the 1 in 2, 5, 10, 20, 50, and 100 year return level (RL) of the maximum change in capacity factor in a 6 hour window and the Offshore North region for each warming level (WL) of interest. In each case, the Bayesian posterior mean (best estimate) is given, with the 95% credible interval around this shown in brackets. These values summarise the curve shown in Figure 11 (c).

WL (°C)	RL:2 years	RL:5 years	RL:10 years	RL:20 years	RL:50 years	RL:100 years
1.20	89.1 (88.8,89.4)	90.6 (90.3,91)	91.6 (91.2,92)	92.4 (91.9,92.9)	93.2 (92.8,93.7)	93.8 (93.3,94.3)
1.50	89.1 (88.9,89.4)	90.7 (90.3,91.1)	91.6 (91.2,92.1)	92.4 (92,92.9)	93.3 (92.8,93.8)	93.8 (93.3,94.3)
2.00	89.1 (88.9,89.5)	90.7 (90.4,91.1)	91.7 (91.3,92.1)	92.5 (92,92.9)	93.3 (92.8,93.8)	93.9 (93.4,94.4)
3.00	89.2 (88.9,89.6)	90.8 (90.4,91.2)	91.8 (91.3,92.2)	92.6 (92.1,93.1)	93.5 (92.9,94)	94 (93.5,94.5)
4.00	89.3 (89,89.6)	90.9 (90.5,91.3)	91.9 (91.4,92.3)	92.7 (92.2,93.2)	93.6 (93,94.1)	94.1 (93.6,94.7)

Table 5: Table summarising the 1 in 2, 5, 10, 20, 50, and 100 year return level (RL) of the maximum change in capacity factor in a 12 hour window and the Offshore North region for each warming level (WL) of interest. In each case, the Bayesian posterior mean (best estimate) is given, with the 95% credible interval around this shown in brackets. These values summarise the curve shown in Figure 11 (d).

WL (°C)	RL:2 years	RL:5 years	RL:10 years	RL:20 years	RL:50 years	RL:100 years
1.20	93.1 (92.9,93.2)	94 (93.9,94.2)	94.6 (94.4,94.9)	95.2 (94.9,95.4)	95.7 (95.5,96)	96.1 (95.8,96.4)
1.50	93.1 (92.9,93.2)	94 (93.8,94.2)	94.6 (94.4,94.9)	95.2 (94.9,95.4)	95.7 (95.4,96)	96.1 (95.8,96.4)
2.00	93.1 (92.9,93.2)	94 (93.8,94.2)	94.6 (94.4,94.9)	95.2 (94.9,95.4)	95.7 (95.4,96)	96.1 (95.8,96.4)
3.00	93.1 (92.9,93.2)	94 (93.8,94.2)	94.6 (94.4,94.9)	95.2 (94.9,95.4)	95.7 (95.4,96)	96.1 (95.8,96.4)
4.00	93.1 (92.9,93.2)	94 (93.8,94.2)	94.6 (94.4,94.9)	95.2 (94.9,95.4)	95.7 (95.4,96)	96.1 (95.8,96.4)

Table 6: Table summarising the 1 in 2, 5, 10, 20, 50, and 100 year return level (RL) of the maximum change in capacity factor in a 24 hour window and the Offshore North region for each warming level (WL) of interest. In each case, the Bayesian posterior mean (best estimate) is given, with the 95% credible interval around this shown in brackets. These values summarise the curve shown in Figure 11 (e).

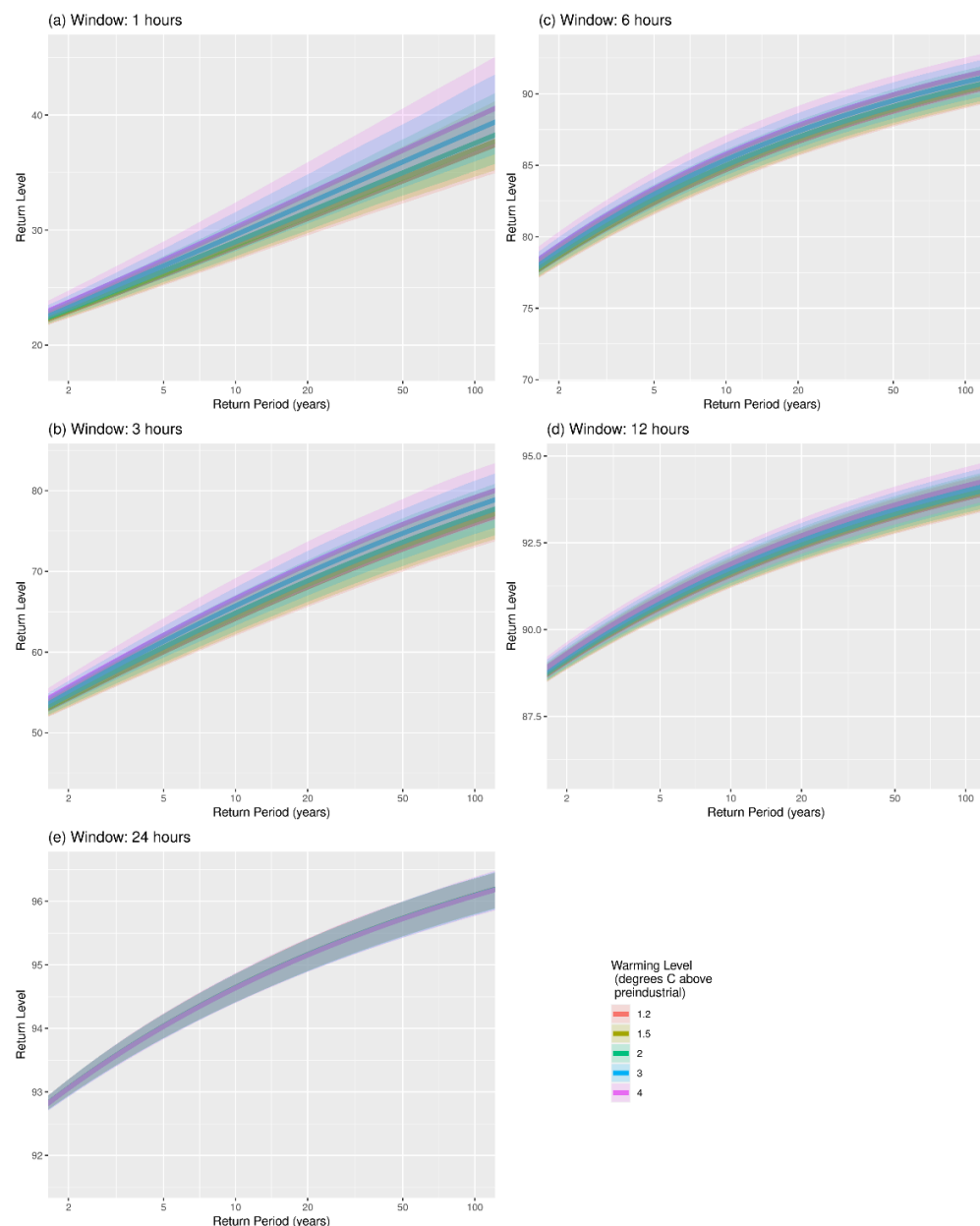


Figure 11: (a) 1 hour, (b) 3 hour, (c) 6 hour, (d) 12 hour and (e) 24 hour Offshore North ramping event return level plots, showing the level of change in capacity factor (on the y axis) associated with a given return period in years (on the x axis), plotted on a logarithmic scale, for five key warming level of interest (shown in different colours). The solid lines represent the return level curves based on the Bayesian posterior mean (i.e. the best estimate), and the shaded areas represent the 95% credible intervals around these best estimates. This means that the true return level has a 95% probability of being within the shaded area.

WL (°C)	RL:2 years	RL:5 years	RL:10 years	RL:20 years	RL:50 years	RL:100 years
1.20	25.8 (24.7,27.2)	30.5 (28.8,32.8)	34.4 (32.2,37.3)	38.4 (35.7,41.9)	43.8 (40.2,48.3)	48 (43.8,53.1)
1.50	25.9 (24.8,27.3)	30.7 (29,33)	34.6 (32.4,37.6)	38.7 (35.9,42.3)	44.3 (40.5,48.8)	48.5 (44.2,53.7)
2.00	26.2 (25,27.6)	31.1 (29.4,33.4)	35.1 (32.8,38.1)	39.3 (36.4,43)	45 (41,49.6)	49.3 (44.8,54.6)
3.00	26.6 (25.4,28.2)	31.8 (30,34.2)	36.1 (33.6,39.2)	40.4 (37.2,44.4)	46.4 (42.2,51.4)	50.9 (46,56.6)
4.00	27.1 (25.8,28.8)	32.6 (30.5,35.2)	37.1 (34.3,40.5)	41.7 (38,45.8)	47.9 (43.3,53.2)	52.6 (47.2,58.7)

Table 7: Table summarising the 1 in 2, 5, 10, 20, 50, and 100 year return level (RL) of the maximum change in capacity factor in a 1 hour window and the Offshore South region for each warming level (WL) of interest. In each case, the Bayesian posterior mean (best estimate) is given, with the 95% credible interval around this shown in brackets. These values summarise the curve shown in Figure 12 (a).

WL (°C)	RL:2 years	RL:5 years	RL:10 years	RL:20 years	RL:50 years	RL:100 years
1.20	50.7 (49.5,52)	55.9 (54.2,57.8)	59.6 (57.5,61.8)	63 (60.7,65.7)	67.1 (64.5,70.2)	69.9 (67.1,73.3)
1.50	50.9 (49.6,52.1)	56.1 (54.4,58)	59.8 (57.8,62.1)	63.3 (61,65.9)	67.4 (64.8,70.5)	70.2 (67.3,73.6)
2.00	51.1 (49.9,52.4)	56.5 (54.7,58.3)	60.3 (58.2,62.5)	63.8 (61.5,66.4)	68 (65.3,71)	70.8 (67.9,74.1)
3.00	51.7 (50.4,53.1)	57.3 (55.4,59.2)	61.2 (59,63.5)	64.8 (62.3,67.5)	69.1 (66.3,72.2)	72 (69,75.3)
4.00	52.2 (50.8,53.8)	58.1 (56.1,60.2)	62.1 (59.7,64.6)	65.8 (63.2,68.7)	70.2 (67.2,73.4)	73.2 (69.9,76.5)

Table 8: Table summarising the 1 in 2, 5, 10, 20, 50, and 100 year return level (RL) of the maximum change in capacity factor in a 3 hour window and the Offshore South region for each warming level (WL) of interest. In each case, the Bayesian posterior mean (best estimate) is given, with the 95% credible interval around this shown in brackets. These values summarise the curve shown in Figure 12 (b).

WL (°C)	RL:2 years	RL:5 years	RL:10 years	RL:20 years	RL:50 years	RL:100 years
1.20	66.4 (65.5,67.2)	70.5 (69.2,71.8)	73.5 (71.9,75)	76.3 (74.5,78)	79.8 (77.6,81.7)	82.1 (79.9,84.2)
1.50	66.5 (65.6,67.4)	70.7 (69.3,71.9)	73.7 (72.1,75.2)	76.5 (74.7,78.2)	80 (77.8,81.9)	82.3 (80.1,84.4)
2.00	66.6 (65.7,67.6)	70.9 (69.5,72.2)	73.9 (72.3,75.5)	76.8 (74.9,78.5)	80.3 (78.2,82.3)	82.7 (80.3,84.7)
3.00	66.9 (65.9,67.9)	71.3 (69.8,72.7)	74.5 (72.7,76.1)	77.4 (75.4,79.3)	80.9 (78.7,83)	83.4 (81,85.5)
4.00	67.3 (66.2,68.3)	71.8 (70.2,73.3)	75 (73.2,76.8)	78 (75.9,80)	81.6 (79.3,83.8)	84 (81.7,86.4)

Table 9: Table summarising the 1 in 2, 5, 10, 20, 50, and 100 year return level (RL) of the maximum change in capacity factor in a 6 hour window and the Offshore South region for each warming level (WL) of interest. In each case, the Bayesian posterior mean (best estimate) is given, with the 95% credible interval around this shown in brackets. These values summarise the curve shown in Figure 12 (c).

WL (°C)	RL:2 years	RL:5 years	RL:10 years	RL:20 years	RL:50 years	RL:100 years
1.20	80.7 (80.1,81.4)	84.1 (83.2,85.1)	86.5 (85.4,87.5)	88.6 (87.4,89.7)	91.1 (89.8,92.3)	92.7 (91.3,93.9)
1.50	80.8 (80.2,81.5)	84.3 (83.3,85.2)	86.6 (85.5,87.7)	88.8 (87.6,89.9)	91.2 (90,92.4)	92.8 (91.5,94)
2.00	81 (80.3,81.7)	84.5 (83.5,85.5)	86.9 (85.7,88)	89 (87.8,90.2)	91.5 (90.2,92.7)	93.1 (91.8,94.3)
3.00	81.3 (80.6,82)	84.9 (84,86)	87.4 (86.2,88.6)	89.6 (88.3,90.8)	92.1 (90.7,93.3)	93.6 (92.3,94.9)
4.00	81.6 (80.8,82.4)	85.4 (84.4,86.5)	88 (86.7,89.2)	90.2 (88.9,91.4)	92.6 (91.2,93.9)	94.2 (92.8,95.4)

Table 10: Table summarising the 1 in 2, 5, 10, 20, 50, and 100 year return level (RL) of the maximum change in capacity factor in a 12 hour window and the Offshore South region for each warming level (WL) of interest. In each case, the Bayesian posterior mean (best estimate) is given, with the 95% credible interval around this shown in brackets. These values summarise the curve shown in Figure 12 (d).

WL (°C)	RL:2 years	RL:5 years	RL:10 years	RL:20 years	RL:50 years	RL:100 years
1.20	90.6 (90.3,90.8)	92 (91.7,92.3)	92.9 (92.5,93.3)	93.6 (93.2,94.1)	94.5 (94,95)	95 (94.5,95.5)
1.50	90.6 (90.4,90.8)	92.1 (91.7,92.4)	93 (92.6,93.4)	93.7 (93.3,94.2)	94.6 (94.1,95.1)	95.1 (94.6,95.6)
2.00	90.7 (90.5,90.9)	92.2 (91.8,92.6)	93.1 (92.7,93.5)	93.9 (93.4,94.4)	94.8 (94.2,95.2)	95.3 (94.7,95.8)
3.00	90.9 (90.6,91.2)	92.5 (92.1,92.8)	93.4 (93,93.9)	94.2 (93.7,94.7)	95.1 (94.5,95.6)	95.7 (95.1,96.2)
4.00	91.1 (90.8,91.4)	92.7 (92.3,93.2)	93.7 (93.2,94.2)	94.6 (94,95.1)	95.5 (94.8,96)	96 (95.4,96.6)

Table 11: Table summarising the 1 in 2, 5, 10, 20, 50, and 100 year return level (RL) of the maximum change in capacity factor in a 24 hour window and the Offshore South region for each warming level (WL) of interest. In each case, the Bayesian posterior mean (best estimate) is given, with the 95% credible interval around this shown in brackets. These values summarise the curve shown in Figure 12 (e).

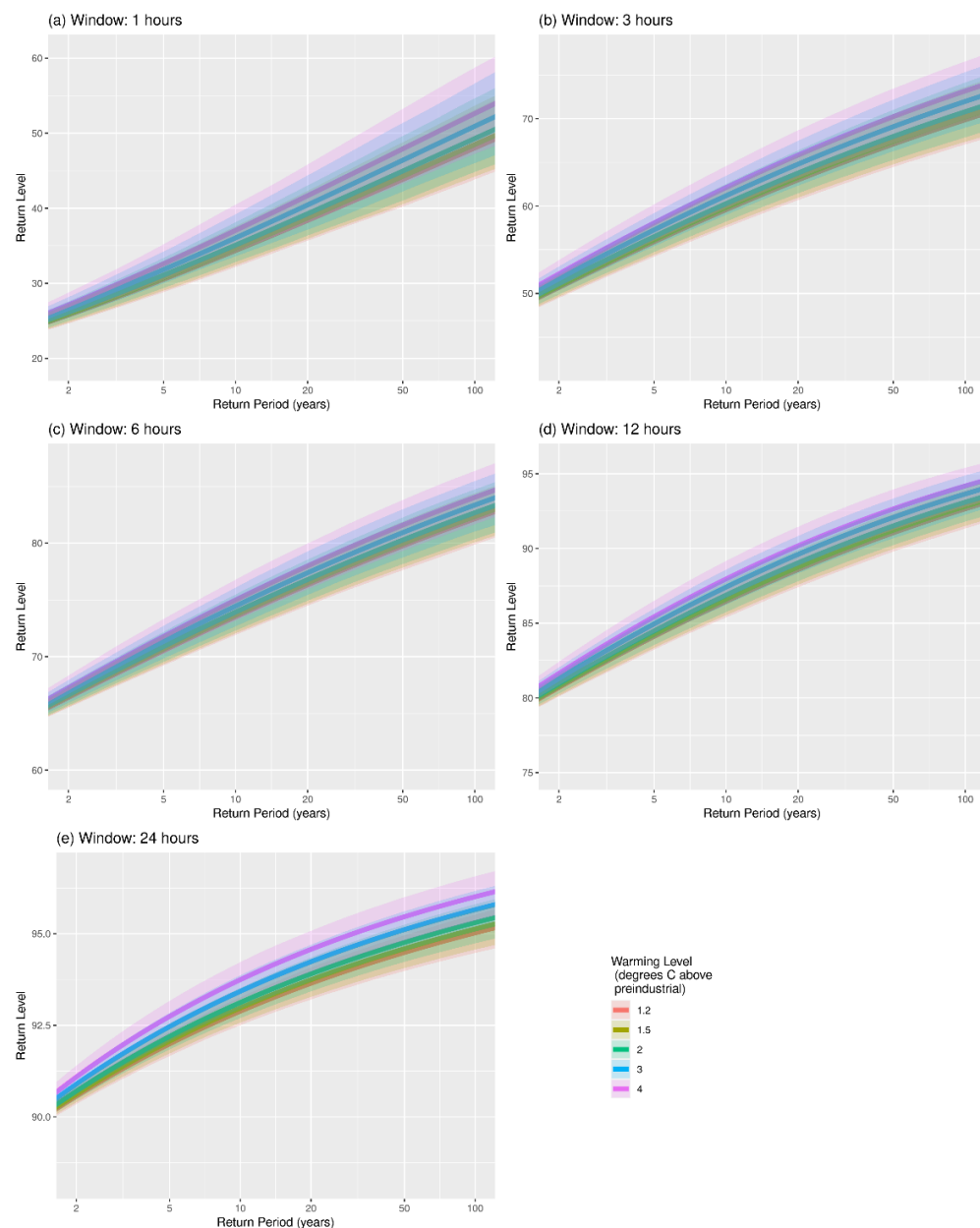


Figure 12: (a) 1 hour, (b) 3 hour, (c) 6 hour, (d) 12 hour and (e) 24 hour Offshore South ramping event return level plots, showing the level of change in capacity factor (on the y axis) associated with a given return period in years (on the x axis), plotted on a logarithmic scale, for five key warming level of interest (shown in different colours). The solid lines represent the return level curves based on the Bayesian posterior mean (i.e. the best estimate), and the shaded areas represent the 95% credible intervals around these best estimates. This means that the true return level has a 95% probability of being within the shaded area.

WL (°C)	RL:2 years	RL:5 years	RL:10 years	RL:20 years	RL:50 years	RL:100 years
1.20	18.7 (18.1,19.4)	21 (20.1,21.9)	22.7 (21.6,23.9)	24.4 (23.1,25.9)	26.7 (25,28.5)	28.4 (26.4,30.6)
1.50	18.7 (18.1,19.3)	20.9 (20.1,21.8)	22.6 (21.6,23.8)	24.4 (23.1,25.8)	26.6 (25,28.4)	28.3 (26.4,30.5)
2.00	18.6 (18.1,19.2)	20.9 (20,21.7)	22.6 (21.5,23.7)	24.3 (22.9,25.6)	26.5 (24.8,28.3)	28.2 (26.2,30.4)
3.00	18.6 (18,19.2)	20.7 (19.9,21.6)	22.4 (21.3,23.5)	24.1 (22.7,25.4)	26.3 (24.6,28)	27.9 (26,29.9)
4.00	18.5 (17.8,19.1)	20.6 (19.7,21.5)	22.2 (21.1,23.4)	23.9 (22.4,25.3)	26.1 (24.3,27.8)	27.7 (25.6,29.8)

Table 12: Table summarising the 1 in 2, 5, 10, 20, 50, and 100 year return level (RL) of the maximum change in capacity factor in a 1 hour window and the Onshore North region for each warming level (WL) of interest. In each case, the Bayesian posterior mean (best estimate) is given, with the 95% credible interval around this shown in brackets. These values summarise the curve shown in Figure 13 (a).

WL (°C)	RL:2 years	RL:5 years	RL:10 years	RL:20 years	RL:50 years	RL:100 years
1.20	43.1 (42,44)	47.1 (45.7,48.5)	50.1 (48.4,51.7)	53 (51.1,55)	56.7 (54.4,59)	59.4 (56.9,61.9)
1.50	43 (42,44)	47.1 (45.7,48.5)	50.1 (48.4,51.7)	53 (51,54.9)	56.7 (54.4,58.9)	59.3 (56.8,61.9)
2.00	42.9 (42,43.9)	47 (45.6,48.4)	49.9 (48.3,51.7)	52.8 (50.9,54.8)	56.5 (54.2,58.8)	59.1 (56.6,61.7)
3.00	42.8 (41.8,43.8)	46.8 (45.3,48.1)	49.7 (47.9,51.4)	52.6 (50.5,54.6)	56.2 (53.7,58.6)	58.8 (56.1,61.4)
4.00	42.7 (41.6,43.7)	46.6 (45,48)	49.5 (47.6,51.2)	52.3 (50.1,54.3)	55.9 (53.2,58.4)	58.5 (55.5,61.2)

Table 13: Table summarising the 1 in 2, 5, 10, 20, 50, and 100 year return level (RL) of the maximum change in capacity factor in a 3 hour window and the Onshore North region for each warming level (WL) of interest. In each case, the Bayesian posterior mean (best estimate) is given, with the 95% credible interval around this shown in brackets. These values summarise the curve shown in Figure 13 (b).

WL (°C)	RL:2 years	RL:5 years	RL:10 years	RL:20 years	RL:50 years	RL:100 years
1.20	64.3 (63.5,65.4)	68 (66.9,69.3)	70.5 (69.2,72)	72.8 (71.3,74.4)	75.5 (73.8,77.5)	77.4 (75.5,79.5)
1.50	64.3 (63.5,65.3)	67.9 (66.8,69.3)	70.4 (69.1,72)	72.7 (71.2,74.4)	75.5 (73.7,77.4)	77.3 (75.4,79.5)
2.00	64.2 (63.4,65.3)	67.8 (66.7,69.2)	70.3 (69,71.9)	72.6 (71.1,74.3)	75.3 (73.6,77.3)	77.2 (75.2,79.4)
3.00	64.1 (63.2,65.1)	67.6 (66.4,69)	70.1 (68.6,71.8)	72.4 (70.7,74.3)	75.1 (73.2,77.2)	76.9 (74.9,79.2)
4.00	64 (63,65.1)	67.5 (66.1,68.9)	69.9 (68.4,71.6)	72.1 (70.4,74.1)	74.8 (72.9,77.1)	76.6 (74.6,79)

Table 14: Table summarising the 1 in 2, 5, 10, 20, 50, and 100 year return level (RL) of the maximum change in capacity factor in a 6 hour window and the Onshore North region for each warming level (WL) of interest. In each case, the Bayesian posterior mean (best estimate) is given, with the 95% credible interval around this shown in brackets. These values summarise the curve shown in Figure 13 (c).

WL (°C)	RL:2 years	RL:5 years	RL:10 years	RL:20 years	RL:50 years	RL:100 years
1.20	77.7 (77.3,78.2)	80.2 (79.6,80.9)	81.9 (81.2,82.7)	83.3 (82.5,84.2)	84.9 (84,86)	86 (85,87.1)
1.50	77.7 (77.3,78.2)	80.2 (79.6,80.9)	81.9 (81.1,82.7)	83.3 (82.5,84.2)	84.9 (84,86)	86 (85,87.1)
2.00	77.7 (77.2,78.2)	80.2 (79.6,80.9)	81.9 (81.1,82.7)	83.3 (82.4,84.2)	84.9 (83.9,86)	86 (84.9,87.1)
3.00	77.7 (77.2,78.2)	80.2 (79.5,81)	81.8 (81,82.7)	83.3 (82.3,84.3)	84.9 (83.8,86)	85.9 (84.7,87.1)
4.00	77.7 (77.1,78.3)	80.2 (79.4,81)	81.8 (80.9,82.8)	83.2 (82.2,84.3)	84.8 (83.6,86.1)	85.9 (84.6,87.2)

Table 15: Table summarising the 1 in 2, 5, 10, 20, 50, and 100 year return level (RL) of the maximum change in capacity factor in a 12 hour window and the Onshore North region for each warming level (WL) of interest. In each case, the Bayesian posterior mean (best estimate) is given, with the 95% credible interval around this shown in brackets. These values summarise the curve shown in Figure 13 (d).

WL (°C)	RL:2 years	RL:5 years	RL:10 years	RL:20 years	RL:50 years	RL:100 years
1.20	83.9 (83.8,84)	85.3 (85.1,85.6)	86.3 (86,86.6)	87 (86.7,87.5)	87.9 (87.5,88.4)	88.5 (88,89.1)
1.50	83.9 (83.8,84.1)	85.3 (85.1,85.6)	86.3 (86,86.6)	87 (86.7,87.5)	87.9 (87.5,88.5)	88.5 (88,89.1)
2.00	83.9 (83.8,84.1)	85.3 (85.1,85.6)	86.3 (85.9,86.6)	87 (86.7,87.5)	87.9 (87.5,88.5)	88.5 (88,89.1)
3.00	83.9 (83.8,84.1)	85.3 (85.1,85.7)	86.2 (85.9,86.7)	87 (86.6,87.6)	87.9 (87.4,88.6)	88.5 (87.9,89.2)
4.00	83.9 (83.8,84.1)	85.3 (85.1,85.7)	86.2 (85.9,86.8)	87 (86.6,87.7)	87.9 (87.4,88.7)	88.5 (87.9,89.3)

Table 16: Table summarising the 1 in 2, 5, 10, 20, 50, and 100 year return level (RL) of the maximum change in capacity factor in a 24 hour window and the Onshore North region for each warming level (WL) of interest. In each case, the Bayesian posterior mean (best estimate) is given, with the 95% credible interval around this shown in brackets. These values summarise the curve shown in Figure 13 (e).

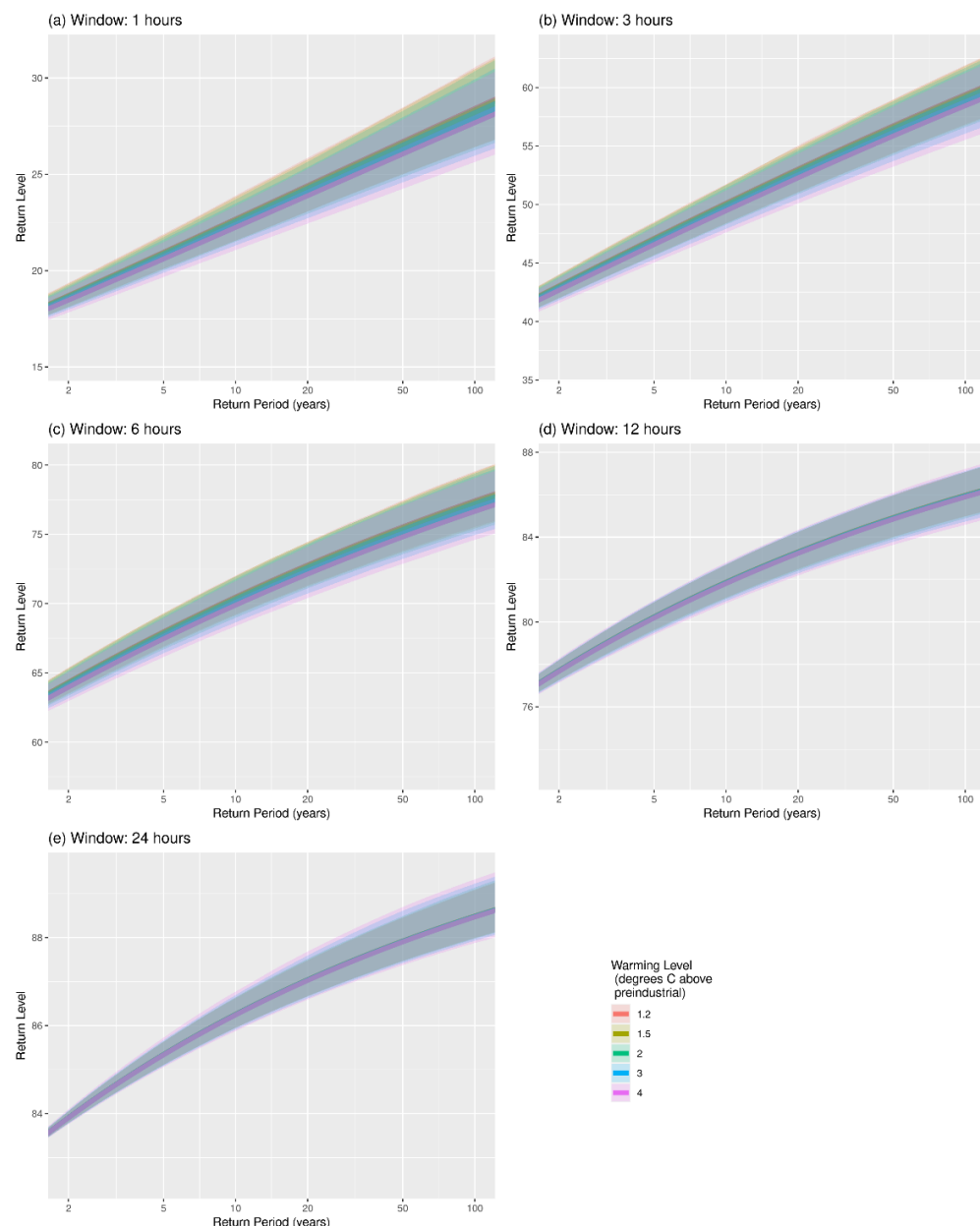


Figure 13: (a) 1 hour, (b) 3 hour, (c) 6 hour, (d) 12 hour and (e) 24 hour Onshore North ramping event return level plots, showing the level of change in capacity factor (on the y axis) associated with a given return period in years (on the x axis), plotted on a logarithmic scale, for five key warming level of interest (shown in different colours). The solid lines represent the return level curves based on the Bayesian posterior mean (i.e. the best estimate), and the shaded areas represent the 95% credible intervals around these best estimates. This means that the true return level has a 95% probability of being within the shaded area.

WL (°C)	RL:2 years	RL:5 years	RL:10 years	RL:20 years	RL:50 years	RL:100 years
1.20	22.3 (21.6,23.2)	25 (24,26.3)	27 (25.8,28.6)	29 (27.6,30.9)	31.7 (30,34)	33.7 (31.8,36.4)
1.50	22.2 (21.6,23.2)	24.9 (23.9,26.2)	26.9 (25.7,28.5)	28.9 (27.5,30.8)	31.6 (29.9,33.9)	33.6 (31.6,36.2)
2.00	22.1 (21.5,23)	24.8 (23.8,26)	26.7 (25.6,28.3)	28.7 (27.4,30.6)	31.4 (29.7,33.6)	33.3 (31.5,35.9)
3.00	22 (21.3,22.8)	24.5 (23.6,25.7)	26.4 (25.3,27.9)	28.4 (27.1,30.1)	30.9 (29.3,33.1)	32.9 (30.9,35.3)
4.00	21.8 (21.2,22.6)	24.3 (23.3,25.4)	26.2 (25,27.5)	28 (26.7,29.7)	30.5 (28.8,32.6)	32.4 (30.4,34.7)

Table 17: Table summarising the 1 in 2, 5, 10, 20, 50, and 100 year return level (RL) of the maximum change in capacity factor in a 1 hour window and the Onshore East region for each warming level (WL) of interest. In each case, the Bayesian posterior mean (best estimate) is given, with the 95% credible interval around this shown in brackets. These values summarise the curve shown in Figure 14 (a).

WL (°C)	RL:2 years	RL:5 years	RL:10 years	RL:20 years	RL:50 years	RL:100 years
1.20	47.1 (45.9,48.3)	51.3 (49.8,53)	54.4 (52.7,56.4)	57.4 (55.5,59.6)	61.2 (59,63.7)	63.9 (61.5,66.7)
1.50	47.1 (45.9,48.3)	51.3 (49.8,53)	54.4 (52.7,56.3)	57.4 (55.4,59.6)	61.1 (58.9,63.7)	63.8 (61.4,66.6)
2.00	47.1 (45.9,48.3)	51.2 (49.7,52.9)	54.3 (52.6,56.3)	57.3 (55.3,59.5)	61 (58.8,63.6)	63.7 (61.3,66.6)
3.00	47 (45.8,48.3)	51.1 (49.6,52.9)	54.2 (52.4,56.3)	57.1 (55.1,59.5)	60.8 (58.6,63.6)	63.5 (61,66.5)
4.00	46.9 (45.7,48.3)	51 (49.5,52.9)	54 (52.2,56.3)	57 (54.9,59.6)	60.6 (58.2,63.6)	63.3 (60.6,66.5)

Table 18: Table summarising the 1 in 2, 5, 10, 20, 50, and 100 year return level (RL) of the maximum change in capacity factor in a 3 hour window and the Onshore East region for each warming level (WL) of interest. In each case, the Bayesian posterior mean (best estimate) is given, with the 95% credible interval around this shown in brackets. These values summarise the curve shown in Figure 14 (b).

WL (°C)	RL:2 years	RL:5 years	RL:10 years	RL:20 years	RL:50 years	RL:100 years
1.20	68.5 (67.5,69.6)	72.4 (71.1,73.8)	75 (73.5,76.6)	77.3 (75.7,79)	80 (78.2,81.8)	81.8 (79.8,83.7)
1.50	68.5 (67.5,69.6)	72.4 (71,73.8)	75 (73.5,76.5)	77.3 (75.6,79)	80 (78.2,81.8)	81.7 (79.8,83.7)
2.00	68.5 (67.4,69.6)	72.4 (71,73.7)	74.9 (73.4,76.5)	77.2 (75.6,78.9)	79.9 (78.1,81.7)	81.7 (79.7,83.6)
3.00	68.4 (67.3,69.5)	72.3 (70.9,73.7)	74.8 (73.3,76.4)	77.1 (75.4,78.8)	79.8 (77.9,81.6)	81.6 (79.5,83.4)
4.00	68.3 (67.2,69.5)	72.2 (70.7,73.7)	74.8 (73.1,76.4)	77.1 (75.2,78.8)	79.7 (77.7,81.6)	81.5 (79.3,83.4)

Table 19: Table summarising the 1 in 2, 5, 10, 20, 50, and 100 year return level (RL) of the maximum change in capacity factor in a 6 hour window and the Onshore East region for each warming level (WL) of interest. In each case, the Bayesian posterior mean (best estimate) is given, with the 95% credible interval around this shown in brackets. These values summarise the curve shown in Figure 14 (c).

WL (°C)	RL:2 years	RL:5 years	RL:10 years	RL:20 years	RL:50 years	RL:100 years
1.20	81.4 (81,82)	83.8 (83.3,84.6)	85.3 (84.7,86.2)	86.6 (85.9,87.5)	88 (87.3,89)	88.9 (88.1,89.9)
1.50	81.4 (81,82)	83.9 (83.3,84.7)	85.4 (84.8,86.3)	86.7 (86,87.6)	88.1 (87.3,89.1)	88.9 (88.1,90)
2.00	81.5 (81.1,82.1)	84 (83.4,84.8)	85.5 (84.8,86.4)	86.8 (86.1,87.7)	88.2 (87.4,89.2)	89 (88.2,90.1)
3.00	81.6 (81.2,82.3)	84.1 (83.5,85)	85.7 (85,86.7)	87 (86.2,88)	88.4 (87.6,89.5)	89.3 (88.4,90.4)
4.00	81.7 (81.2,82.4)	84.3 (83.6,85.2)	85.9 (85.1,86.9)	87.2 (86.4,88.3)	88.6 (87.7,89.8)	89.5 (88.5,90.7)

Table 20: Table summarising the 1 in 2, 5, 10, 20, 50, and 100 year return level (RL) of the maximum change in capacity factor in a 12 hour window and the Onshore East region for each warming level (WL) of interest. In each case, the Bayesian posterior mean (best estimate) is given, with the 95% credible interval around this shown in brackets. These values summarise the curve shown in Figure 14 (d).

WL (°C)	RL:2 years	RL:5 years	RL:10 years	RL:20 years	RL:50 years	RL:100 years
1.20	88.4 (88.2,88.5)	89.6 (89.4,89.8)	90.3 (90.1,90.6)	90.9 (90.6,91.2)	91.5 (91.2,91.8)	91.8 (91.5,92.2)
1.50	88.4 (88.2,88.5)	89.6 (89.4,89.8)	90.3 (90.0,90.6)	90.9 (90.6,91.1)	91.4 (91.1,91.8)	91.8 (91.5,92.2)
2.00	88.3 (88.2,88.5)	89.6 (89.3,89.8)	90.3 (90.0,90.5)	90.8 (90.6,91.1)	91.4 (91.1,91.7)	91.8 (91.4,92.1)
3.00	88.3 (88.2,88.5)	89.5 (89.3,89.8)	90.2 (89.9,90.5)	90.8 (90.5,91.1)	91.4 (91.1,91.7)	91.7 (91.3,92.1)
4.00	88.3 (88.1,88.4)	89.5 (89.2,89.7)	90.2 (89.9,90.5)	90.7 (90.4,91.1)	91.3 (90.9,91.7)	91.6 (91.3,92.1)

Table 21: Table summarising the 1 in 2, 5, 10, 20, 50, and 100 year return level (RL) of the maximum change in capacity factor in a 24 hour window and the Onshore East region for each warming level (WL) of interest. In each case, the Bayesian posterior mean (best estimate) is given, with the 95% credible interval around this shown in brackets. These values summarise the curve shown in Figure 14 (e).

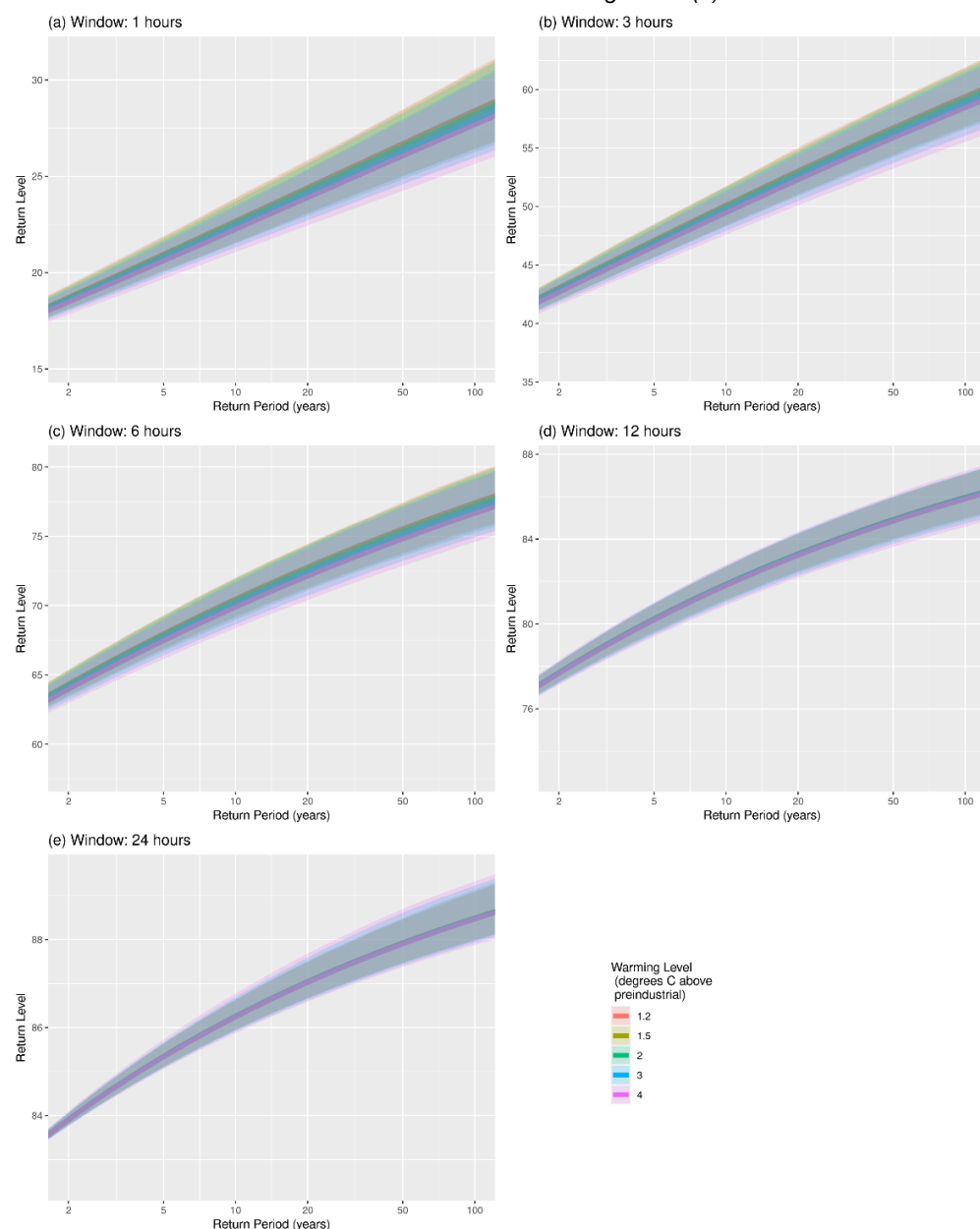


Figure 14: (a) 1 hour, (b) 3 hour, (c) 6 hour, (d) 12 hour and (e) 24 hour Onshore East ramping event return level plots, showing the level of change in capacity factor (on the y axis) associated with a given return period in years (on the x axis), plotted on a logarithmic scale, for five key warming level of interest (shown in different colours). The solid lines represent the return level curves based on the Bayesian posterior mean (i.e. the best estimate), and the shaded areas represent the 95% credible intervals around these best estimates. This means that the true return level has a 95% probability of being within the shaded area.

WL (°C)	RL:2 years	RL:5 years	RL:10 years	RL:20 years	RL:50 years	RL:100 years
1.20	20.9 (20.3,21.9)	23.3 (22.5,24.6)	25.1 (24.1,26.7)	26.9 (25.7,28.7)	29.2 (27.8,31.4)	31 (29.3,33.4)
1.50	20.9 (20.3,21.9)	23.3 (22.5,24.6)	25.1 (24.1,26.7)	26.9 (25.7,28.7)	29.3 (27.8,31.4)	31 (29.3,33.4)
2.00	20.9 (20.3,21.8)	23.3 (22.5,24.6)	25.1 (24.1,26.7)	26.9 (25.7,28.7)	29.3 (27.8,31.4)	31 (29.3,33.4)
3.00	20.9 (20.3,21.9)	23.3 (22.4,24.6)	25.1 (24.1,26.7)	26.9 (25.7,28.7)	29.3 (27.8,31.4)	31.1 (29.3,33.4)
4.00	20.9 (20.3,21.9)	23.3 (22.4,24.6)	25.2 (24,26.7)	27 (25.6,28.7)	29.4 (27.7,31.4)	31.1 (29.3,33.5)

Table 22: Table summarising the 1 in 2, 5, 10, 20, 50, and 100 year return level (RL) of the maximum change in capacity factor in a 1 hour window and the Onshore West region for each warming level (WL) of interest. In each case, the Bayesian posterior mean (best estimate) is given, with the 95% credible interval around this shown in brackets. These values summarise the curve shown in Figure 15 (a).

WL (°C)	RL:2 years	RL:5 years	RL:10 years	RL:20 years	RL:50 years	RL:100 years
1.20	44.1 (43,45.1)	48.2 (46.7,49.6)	51.2 (49.4,52.8)	54.2 (52.1,56)	57.9 (55.5,60.1)	60.6 (58.1,63.1)
1.50	44.1 (43,45.1)	48.2 (46.6,49.6)	51.2 (49.4,52.8)	54.1 (52,56)	57.9 (55.5,60.1)	60.6 (58,63.1)
2.00	44.1 (43,45)	48.1 (46.6,49.6)	51.2 (49.3,52.8)	54.1 (52,56)	57.9 (55.4,60.1)	60.6 (57.9,63.1)
3.00	44 (42.9,45)	48.1 (46.5,49.5)	51.1 (49.3,52.8)	54.1 (51.9,56)	57.8 (55.2,60)	60.5 (57.7,63)
4.00	44 (42.8,45)	48.1 (46.4,49.4)	51.1 (49.1,52.7)	54 (51.6,55.9)	57.7 (55,60)	60.4 (57.5,63)

Table 23: Table summarising the 1 in 2, 5, 10, 20, 50, and 100 year return level (RL) of the maximum change in capacity factor in a 3 hour window and the Onshore West region for each warming level (WL) of interest. In each case, the Bayesian posterior mean (best estimate) is given, with the 95% credible interval around this shown in brackets. These values summarise the curve shown in Figure 15 (b).

WL (°C)	RL:2 years	RL:5 years	RL:10 years	RL:20 years	RL:50 years	RL:100 years
1.20	65.4 (64.7,66.4)	69.4 (68.4,70.8)	72.2 (71,73.8)	74.8 (73.4,76.5)	77.9 (76.4,79.9)	80 (78.3,82.1)
1.50	65.5 (64.8,66.5)	69.5 (68.5,70.8)	72.3 (71,73.8)	74.9 (73.4,76.6)	78 (76.4,80)	80.1 (78.4,82.2)
2.00	65.5 (64.8,66.5)	69.6 (68.5,70.9)	72.4 (71.1,73.9)	75 (73.5,76.8)	78.1 (76.5,80.1)	80.2 (78.4,82.3)
3.00	65.7 (64.8,66.6)	69.7 (68.6,71.2)	72.6 (71.1,74.3)	75.2 (73.6,77.1)	78.3 (76.5,80.5)	80.5 (78.5,82.7)
4.00	65.8 (64.8,66.9)	69.9 (68.5,71.5)	72.8 (71.1,74.6)	75.4 (73.6,77.5)	78.6 (76.5,80.9)	80.7 (78.4,83.2)

Table 24: Table summarising the 1 in 2, 5, 10, 20, 50, and 100 year return level (RL) of the maximum change in capacity factor in a 6 hour window and the Onshore West region for each warming level (WL) of interest. In each case, the Bayesian posterior mean (best estimate) is given, with the 95% credible interval around this shown in brackets. These values summarise the curve shown in Figure 15 (c).

WL (°C)	RL:2 years	RL:5 years	RL:10 years	RL:20 years	RL:50 years	RL:100 years
1.20	81 (80.5,81.6)	83.5 (82.8,84.2)	85 (84.2,85.7)	86.3 (85.4,87.1)	87.7 (86.8,88.6)	88.6 (87.6,89.6)
1.50	81 (80.5,81.5)	83.5 (82.8,84.1)	85 (84.2,85.7)	86.3 (85.4,87.1)	87.7 (86.8,88.6)	88.6 (87.6,89.5)
2.00	81 (80.5,81.5)	83.4 (82.7,84.1)	84.9 (84.1,85.8)	86.2 (85.4,87.1)	87.6 (86.7,88.6)	88.5 (87.5,89.5)
3.00	80.9 (80.4,81.5)	83.3 (82.6,84.1)	84.8 (84,85.7)	86.1 (85.2,87.1)	87.5 (86.6,88.6)	88.4 (87.4,89.5)
4.00	80.9 (80.3,81.5)	83.3 (82.6,84.1)	84.8 (83.9,85.7)	86 (85.1,87.1)	87.4 (86.4,88.5)	88.3 (87.2,89.5)

Table 25: Table summarising the 1 in 2, 5, 10, 20, 50, and 100 year return level (RL) of the maximum change in capacity factor in a 12 hour window and the Onshore West region for each warming level (WL) of interest. In each case, the Bayesian posterior mean (best estimate) is given, with the 95% credible interval around this shown in brackets. These values summarise the curve shown in Figure 15 (d).

WL (°C)	RL:2 years	RL:5 years	RL:10 years	RL:20 years	RL:50 years	RL:100 years
1.20	87.2 (87.1,87.4)	88.6 (88.3,88.8)	89.4 (89.1,89.7)	90 (89.7,90.3)	90.7 (90.3,91)	91.1 (90.6,91.5)
1.50	87.2 (87.1,87.4)	88.6 (88.4,88.8)	89.4 (89.1,89.7)	90 (89.7,90.4)	90.7 (90.3,91.1)	91.1 (90.7,91.5)
2.00	87.3 (87.1,87.4)	88.6 (88.4,88.9)	89.4 (89.1,89.8)	90.1 (89.7,90.4)	90.8 (90.4,91.1)	91.2 (90.7,91.6)
3.00	87.3 (87.2,87.5)	88.7 (88.4,89)	89.5 (89.2,89.9)	90.2 (89.8,90.6)	90.9 (90.4,91.3)	91.3 (90.8,91.8)
4.00	87.4 (87.2,87.5)	88.8 (88.5,89.1)	89.7 (89.3,90)	90.3 (89.9,90.7)	91 (90.5,91.5)	91.4 (90.9,91.9)

Table 26: Table summarising the 1 in 2, 5, 10, 20, 50, and 100 year return level (RL) of the maximum change in capacity factor in a 24 hour window and the Onshore West region for each warming level (WL) of interest. In each case, the Bayesian posterior mean (best estimate) is given, with the 95% credible interval around this shown in brackets. These values summarise the curve shown in Figure 15 (e).

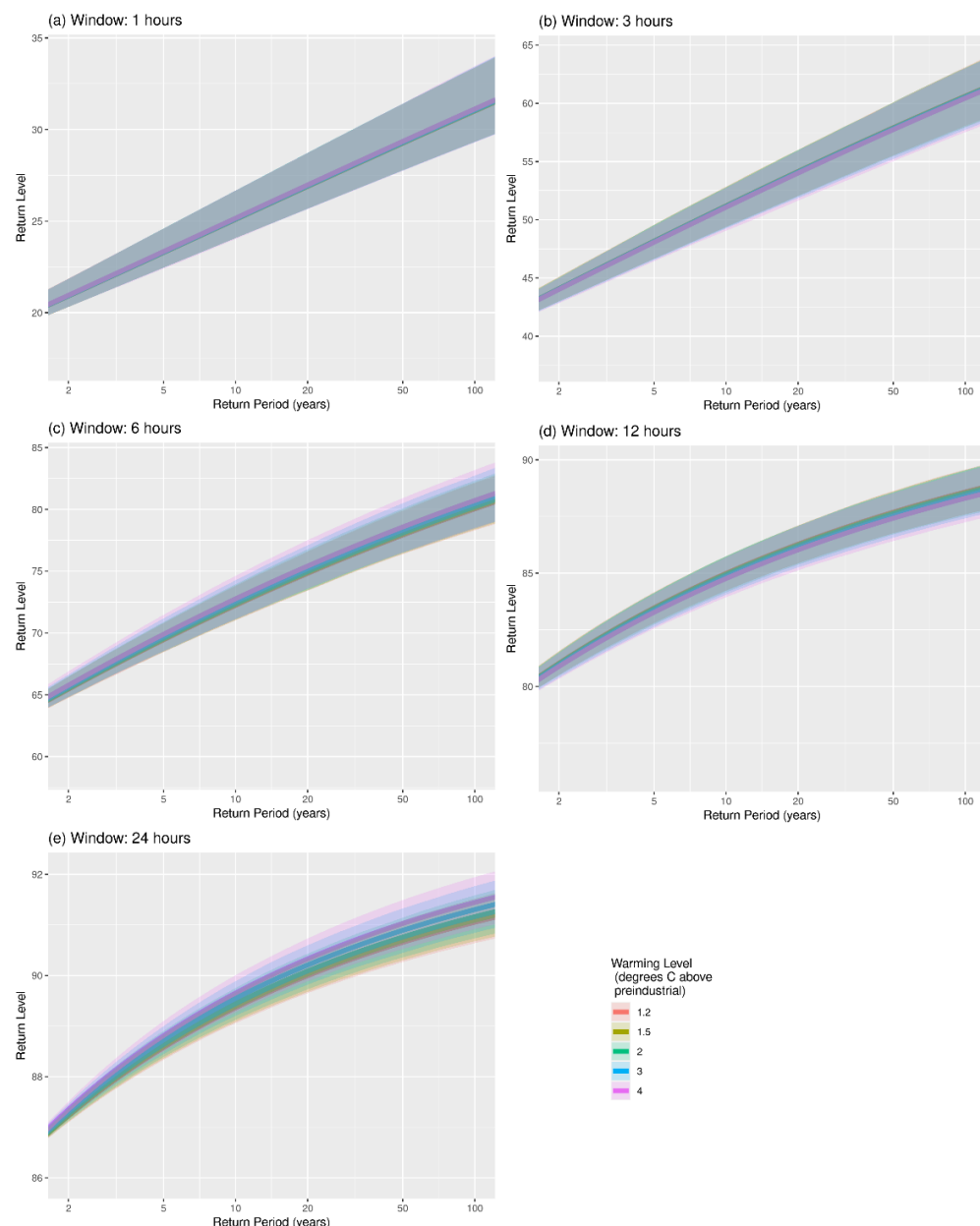


Figure 15: (a) 1 hour, (b) 3 hour, (c) 6 hour, (d) 12 hour and (e) 24 hour Onshore West ramping event return level plots, showing the level of change in capacity factor (on the y axis) associated with a given return period in years (on the x axis), plotted on a logarithmic scale, for five key warming level of interest (shown in different colours). The solid lines represent the return level curves based on the Bayesian posterior mean (i.e. the best estimate), and the shaded areas represent the 95% credible intervals around these best estimates. This means that the true return level has a 95% probability of being within the shaded area.

3.5 Selecting adverse weather scenarios for the final dataset

This section describes the approach used to select relevant adverse weather scenarios for the final dataset. These scenarios are selected from the calibrated UKCP18 100m wind speed data. UKCP18 is used rather than Euro4 as the 240 model years as opposed to 36 historical years means that many more examples of each type of event are available and so can represent a wider range of possible short-duration adverse weather scenarios. This was deemed to be an important feature of the final dataset (Pearce et al., 2021) as this is more likely to capture events which are relevant for various sub-regions of the five defined regions that this analysis is based upon.

Adverse weather scenarios are selected to represent:

1. Each length of time window: 1-, 3-, 6-, 12- and 24-hour;
2. In each region: Offshore North, Offshore South, Onshore North, Onshore East and Onshore West as defined in Figure 1;
3. For a number of extreme levels: 1 in 2, 5, 10, 20, 50 and 100 year return levels;

In terms of the maximum change in capacity factor, as defined in Section 2. This is at the current day (1.2°C), above pre-industrial global mean temperature, as the return levels of the higher warming levels were not found to be materially different to those at current day.

In each case, the UKCP18 adverse weather scenarios are selected based on the EVA results shown in Table 2 - Table 26. Specifically, this is based on the uncertainty range associated with that given combination of event characteristics (event window, region and return level). For example, adverse weather scenarios selected for the final dataset to represent 6-hour Offshore South ramping events with a return period of 100 years, are selected from those identified as having a maximum change in capacity factor in the range of 79.9-84.2 (see Table 9).

For each combination of event characteristics, up to 10 events are selected from the UKCP18 record. These events are sampled randomly from the events identified for the selected time window that fall within the relevant range of extremity (so for 6-hour Offshore South events with a return period of 100 years, this would be 6-hour events with a maximum change in capacity factor between 79.9 and 84.2. There are 6 event combinations where there are less than 10 examples, and in this case all appropriate events will be shared. The event types and return periods where this occurs are shown in Table 27.

Time Window	Region	Return Period	Number of Events
1-hour	Onshore East	1 in 100 years	6
1-hour	Offshore South	1 in 100 years	9
6-hour	Onshore East	1 in 100 years	9
12-hour	Onshore North	1 in 100 years	5
12-hour	Onshore West	1 in 100 years	9
24-hour	Onshore North	1 in 50 years	9

Table 27: List of the event types and return periods where less than 10 relevant examples were available in the UKCP18 record. The number of events of this type that are selected (all available) is shown in the fourth column.

Based on this selection method, a total of 1381 short-duration adverse weather scenarios are selected and included within the final dataset of 'Adverse Weather Scenarios for Future Electricity Systems'. For each selected event, the associated 100m wind speed is provided within the final dataset. These data have been bias corrected and processed as outlined in Section 3.2.1 and Section 3.2.2.

4 The Adverse Weather Scenarios for Future Electricity Systems dataset

4.1 Existing available dataset (long-duration events)

Phase 2 of the project developed a dataset of long-duration adverse weather scenarios. This dataset characterises winter-time and summer-time wind-drought-peak-demand events, and summertime surplus generation events, in the UK and in Europe. It contains gridded daily average meteorological data (surface temperature, 100m wind speed and surface solar radiation) associated with a range of examples of such events, capturing various extreme levels (1 in 2, 5, 10, 20, 50 and 100 year return period events) and climate warming levels (current day, 1.5°C, 2°C, 3°C and 4°C above preindustrial levels).

4.2 Updates to the dataset (short-duration events)

The short-duration adverse weather scenarios developed in this phase of the project have now been added to the Adverse Weather Scenarios for Future Electricity Systems dataset. This section of the dataset characterises wind generation ramping events over five regions (two offshore and three onshore) of GB. It contains gridded hourly 100m wind speed data associated with a range of examples of these events over five different time windows (1-, 3-, 6-, 12- and 24-hours), capturing various extreme levels (1 in 2, 5, 10, 20, 50 and 100 year return period events) at the current day (1.2°C above preindustrial levels) climate warming.

4.3 Downloading the data

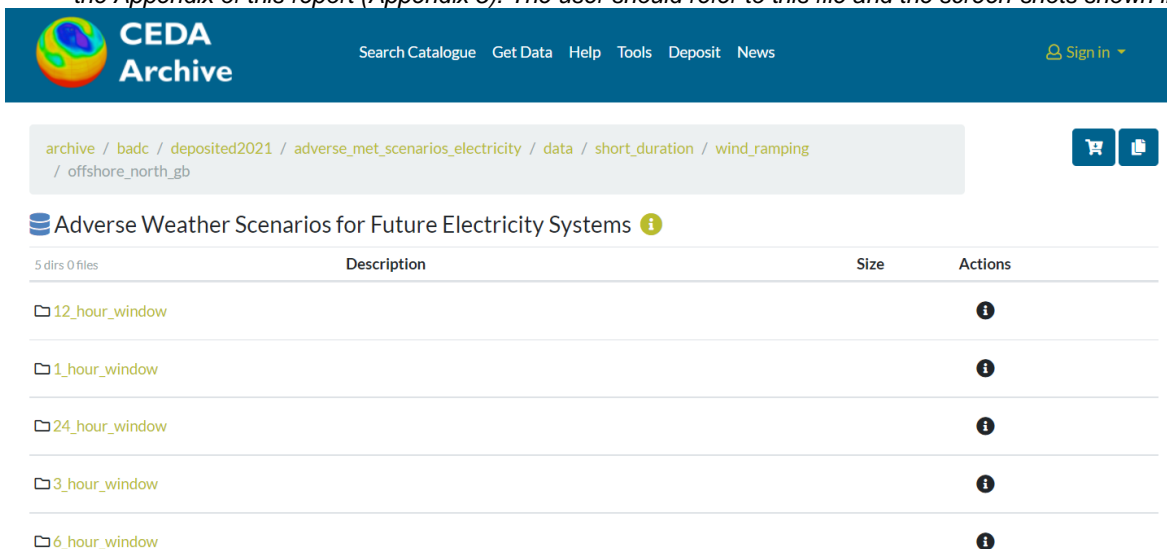
The gridded meteorological data contained within the Adverse Weather Scenarios for Future Electricity Systems dataset can be freely downloaded from the CEDA archive:

- Project record:
<https://catalogue.ceda.ac.uk/uuid/701276b1c63d48e784ba1f3673607628>;
- Dataset record:
<https://catalogue.ceda.ac.uk/uuid/7beeed0bc7fa41feb10be22ee9d10f00>;
- Data repository:
https://data.ceda.ac.uk/badc/deposited2021/adverse_met_scenarios_electricity/data

Downloading the data requires the user to register for a free CEDA account¹². Once registered, the user can download the data from the data repository (accessed using the link provided above). A 'README.txt' file is included within the data repository, explaining the filing system, file naming convention used, and file meta data in detail. A copy of this file is also included in

¹² <https://services.ceda.ac.uk/cedasite/register/info/>

the Appendix of this report (Appendix 5). The user should refer to this file and the screen-shots shown in



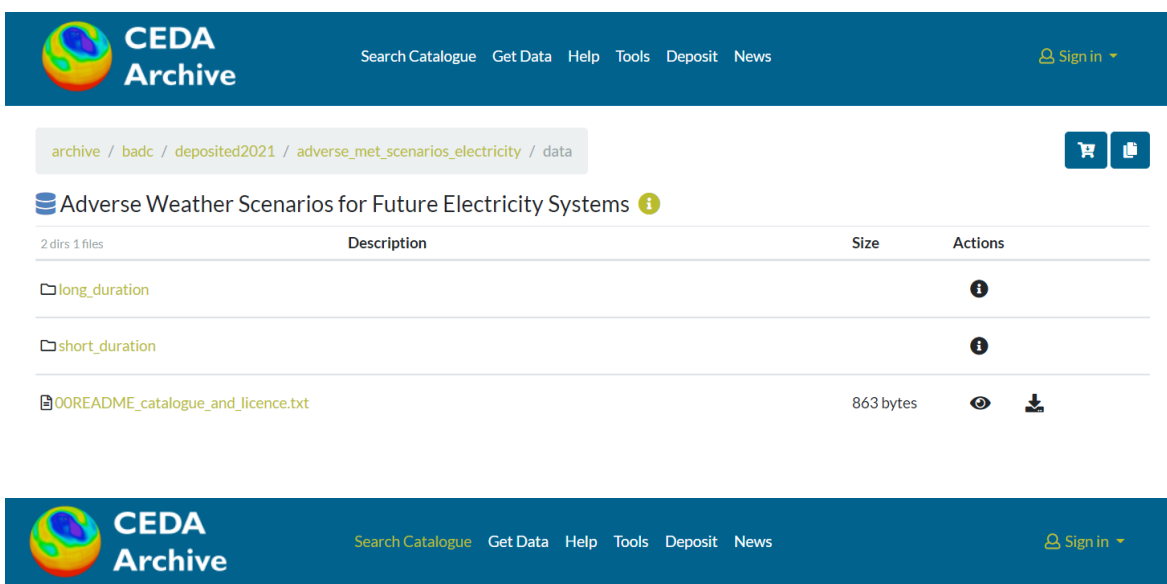
archive / badc / deposited2021 / adverse_met_scenarios_electricity / data / short_duration / wind_ramping / offshore_north_gb

Adverse Weather Scenarios for Future Electricity Systems

5 dirs 0 files	Description	Size	Actions
12_hour_window			i
1_hour_window			i
24_hour_window			i
3_hour_window			i
6_hour_window			i

Figure 16 to Figure 18 when downloading data from the Adverse Weather Scenarios for Future Electricity Systems dataset.

a)

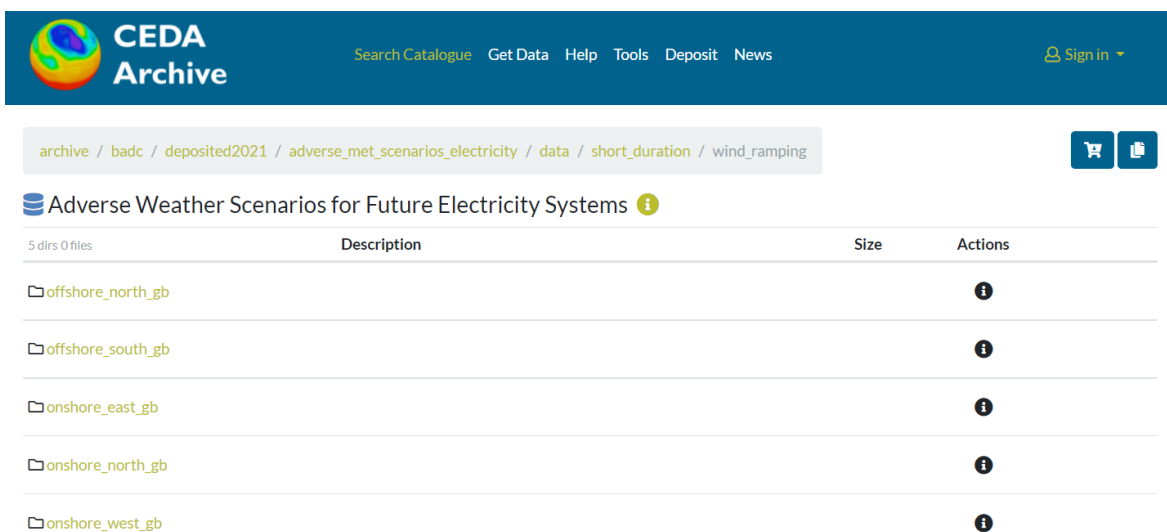


archive / badc / deposited2021 / adverse_met_scenarios_electricity / data

Adverse Weather Scenarios for Future Electricity Systems

2 dirs 1 files	Description	Size	Actions
long_duration			i
short_duration			i
00README_catalogue_and_licence.txt		863 bytes	i d

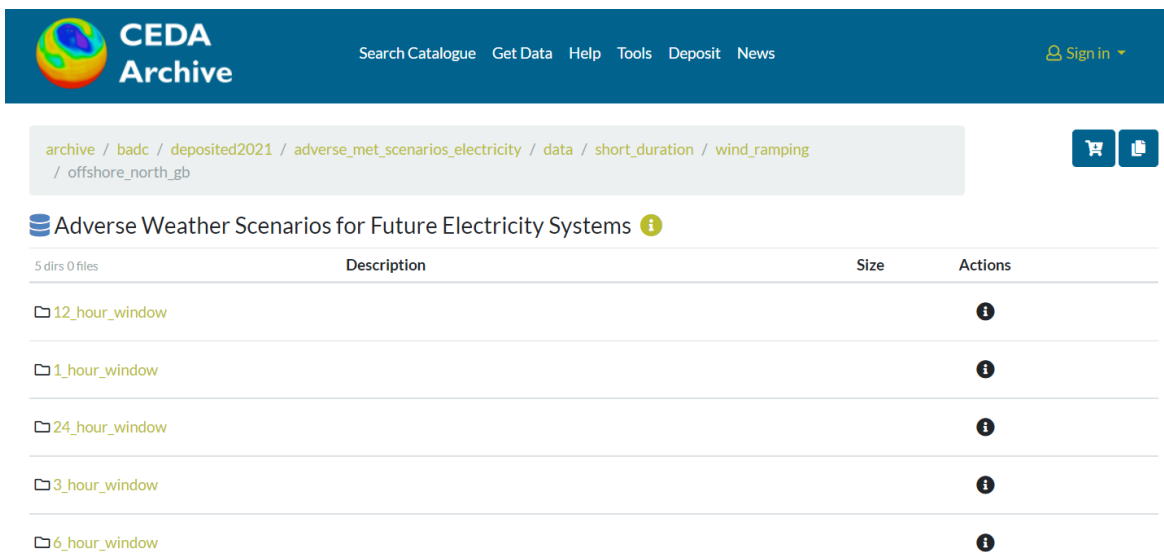
b)



archive / badc / deposited2021 / adverse_met_scenarios_electricity / data / short_duration / wind_ramping

Adverse Weather Scenarios for Future Electricity Systems

5 dirs 0 files	Description	Size	Actions
offshore_north_gb			i
offshore_south_gb			i
onshore_east_gb			i
onshore_north_gb			i
onshore_west_gb			i



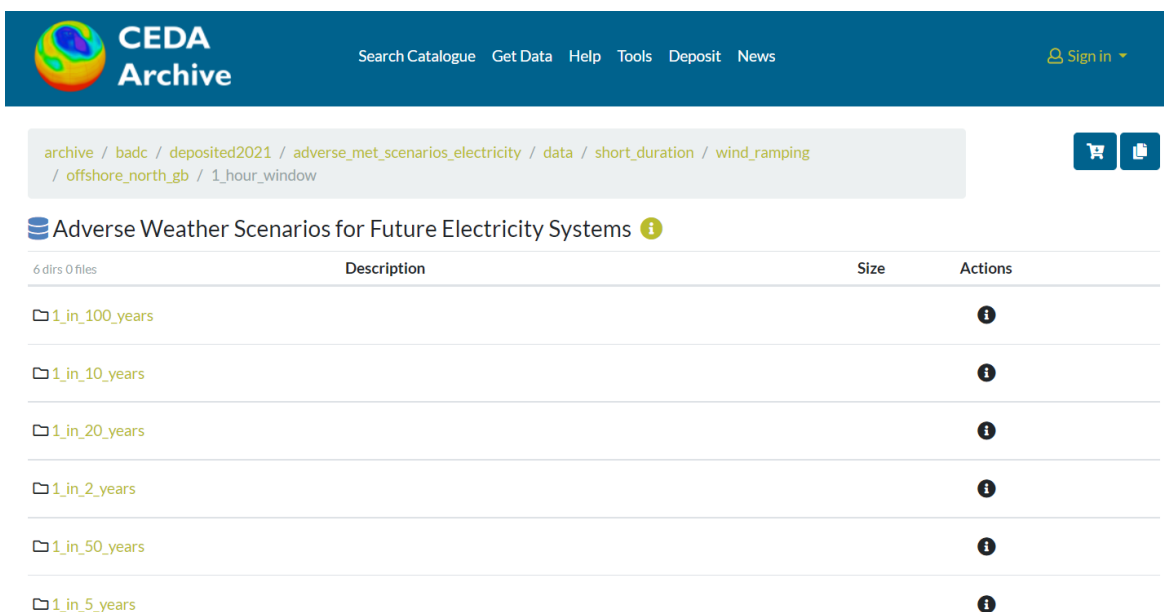
archive / badc / deposited2021 / adverse_met_scenarios_electricity / data / short_duration / wind_ramping / offshore_north_gb

Adverse Weather Scenarios for Future Electricity Systems

5 dirs 0 files	Description	Size	Actions
12_hour_window			i
1_hour_window			i
24_hour_window			i
3_hour_window			i
6_hour_window			i

Figure 16: Screen-shots showing the navigation of the CEDA filing system from the data repository, to reach the gridded meteorological data associated with 'event 1', selected to represent short duration wind ramping events in a 1 hour window and the Offshore North GB region, at a 1 in 100 year return level: Part 1.

d)



archive / badc / deposited2021 / adverse_met_scenarios_electricity / data / short_duration / wind_ramping / offshore_north_gb / 1_hour_window

Adverse Weather Scenarios for Future Electricity Systems













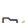



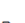



6 dirs 0 files	Description	Size	Actions
1_in_100_years			i
1_in_10_years			i
1_in_20_years			i
1_in_2_years			i
1_in_50_years			i
1_in_5_years			i

Figure 17: Screen-shots showing the navigation of the CEDA filing system from the data repository, to reach the gridded meteorological data associated with 'event 1', selected to represent short duration wind ramping events in a 1 hour window and the Offshore North GB region, at a 1 in 100 year return level: Part 2.

archive / badc / deposited2021 / adverse_met_scenarios_electricity / data / short_duration / wind_ramping / offshore_north_gb / 1_hour_window / 1_in_100_years



Adverse Weather Scenarios for Future Electricity Systems

10 dirs 0 files	Description	Size	Actions
	event1		
	event10		
	event2		
	event3		
	event4		
	event5		
	event6		
	event7		
	event8		
	event9		

archive / badc / deposited2021 / adverse_met_scenarios_electricity / data / short_duration / wind_ramping / offshore_north_gb / 1_hour_window / 1_in_100_years / event1



Adverse Weather Scenarios for Future Electricity Systems


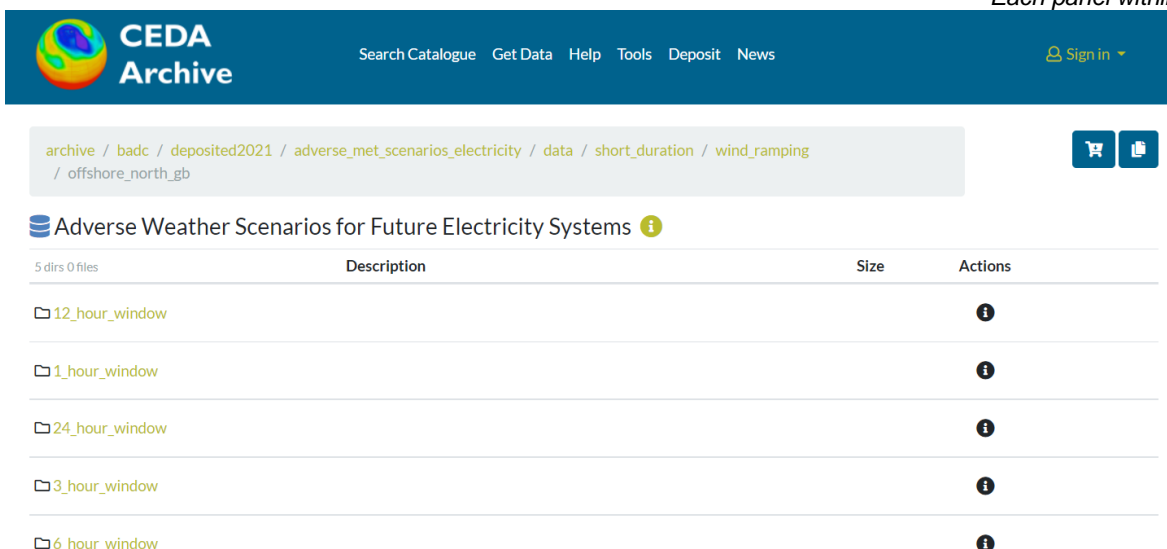
0 dirs 1 files	Description	Size	Actions
	wind_ramping_offshore_north_gb_1_hour_window_1_in_100_years_event1_windspeed.nc	479.5 MB	 

Figure 18: Screen-shots showing the navigation of the CEDA filing system from the data repository, to reach the gridded meteorological data associated with 'event 1', selected to represent short duration wind ramping events in a 1 hour window and the Offshore North GB region, at a 1 in 100 year return level: Part 3.



The screenshot shows the CEDA Archive website. At the top, there is a navigation bar with the CEDA Archive logo, a search bar, and links for Search Catalogue, Get Data, Help, Tools, Deposit, and News. A 'Sign in' button is also present. Below the navigation bar, a breadcrumb trail shows the current directory path: archive / badc / deposited2021 / adverse_met_scenarios_electricity / data / short_duration / wind_ramping / offshore_north_gb. To the right of the path are icons for a shopping cart and a document. Below the path, there is a section titled 'Adverse Weather Scenarios for Future Electricity Systems' with an information icon. Under this title, a table lists sub-directories. The table has four columns: '5 dirs 0 files', 'Description', 'Size', and 'Actions'. The sub-directories listed are 12_hour_window, 1_hour_window, 24_hour_window, 3_hour_window, and 6_hour_window, each with an information icon in the Actions column.

5 dirs 0 files	Description	Size	Actions
12_hour_window			i
1_hour_window			i
24_hour_window			i
3_hour_window			i
6_hour_window			i

Figure 16 to Figure 18 shows a step in the navigation of the CEDA filing system from the data repository, to reach the gridded meteorological data associated with 'event 1', selected to represent 1-hour ramping scenarios in the Offshore North GB region, at a 1 in 100 year return level. Screen-shot (a) shows the full data repository; (b) the sub-directories contained within the 'short_duration' then 'wind_ramping' directory in (a) related to the event region; (c) the sub-directories contained within the 'offshore_north_gb' directory in (b) related to the time window length; (d) the sub-directories contained within the '1_hour_window' directory related to the extreme level (return period); (e) the sub-directories contained within the 'return period 1 in 100 years' directory in (d) related to the event number; (f) the gridded wind speed data (windspeed) contained within 'event 1' .. The file path in each case is shown at the top of the panel, ending at:

'.../short_duration

/wind_ramping/offshore_north_gb/1_hour_window/1_in_100_years/event1'.

An equivalent route can be taken to the gridded data associated each adverse weather scenario contained within the dataset. For example, the gridded meteorological data associated with 'event 1', selected to represent 24-hour wind ramping scenarios in the Onshore West region, at a 1 in 20 year return would be reached via the file path '.../short_duration /wind_ramping/onshore_west_gb/1_in_20 _years/event1'.

Note that the previously shared long-duration adverse weather scenarios can now be found in the 'long_duration' subdirectory. Within this, the file structure remains the same as outlined in (Dawkins et al., 2021b).

Each gridded meteorological data file is provided in a NetCDF format, and in all cases, the start date, duration and severity of the adverse weather event, contained within the time slice of data, are given in the NetCDF global attributes. These are described in more detail in the associated 'README.txt' file contained within the data repository and shown in Appendix 5.

5 Summary and Conclusion

This report has presented the methods developed to produce the short-duration event component of the 'Adverse Weather Scenarios for Future Electricity Systems' dataset. This dataset characterises wind generation ramping events, (a large change in wind generation capacity factor over a short time period) across five onshore and offshore regions of GB. It contains gridded hourly 100m wind speed data associated with a range of examples of these events over five different time windows (1-, 3-, 6-, 12- and 24-hours) capturing various extreme levels (1 in 2, 5, 10, 20, 50 and 100 year return period events) at the present day (1.2°C above preindustrial level) warming level, and are shown to also be representative of events at higher climate warming levels (1.5°C, 2°C, 3°C and 4°C above pre-industrial levels). The dataset, now containing both long and short-duration adverse weather events is freely available to download from the CEDA archive.

A summary of the approach developed to characterise short-duration adverse weather events, specifically the wind generation ramping events which are the focus of this report, was given. Using this method, wind ramping events were identified from historical hindcast (Euro4), and historical climate model hindcast and future climate projection (UKCP18) data. The use of UKCP18 provided 240 additional plausible weather years to better put the historical ramping events identified from Euro4 into context and potentially allow for more extreme events than those which have previously occurred to be represent. It also provided 480 future years to enable the effect of climate change to be explored and assessed.

Before the climate model hindcasts and projections were used to identify short-duration adverse weather scenarios, the associated wind speed data underwent calibration and rigorous validation. This was done to ensure that the climate model data was not biased or missing any information, and that it was suitable to estimate wind generation from (corresponding to same height above ground as wind turbines). Specifically, a univariate variance scaling approach was used to bias correct the model data, and data science generalised additive models were developed to estimate 100m (above ground) wind speed from 10m wind speed. These models have been confirmed to produce calibrated climate model hindcast and future projection data that has characteristics consistent with the historical hindcast data.

Next, the short-duration adverse weather scenarios identified from both data sources were compared graphically. Initially wind ramping events present in the (historical period) climate model hindcast were compared to the events identified from the historical record. In particular

the frequency with which each type of event exceeds a certain magnitude across the two records were compared. A strong agreement between the historical data initially used to characterise short-duration events and the additional historical climate model hindcast data is found regarding the frequency of each type of event. Therefore, there is confidence that the climate model data, in terms of both the historical period and future projections, represents short-term wind fluctuations accurately enough provide good insights on ramping events. It was also found that events more extreme than those identified from the historical record are seen in the historical period of the climate model projections, hence including the climate model historical data in the analysis allows for the exploration of unprecedented meteorological events.

Following this, the ramping events identified from the climate model future projections were compared graphically to the historical events. For some event types, some magnitudes of ramping events were found to occur more frequently in the future projections than in the historical projections however at this stage the increase was not assessed for statistical significance.

A non-stationary statistical extreme value analysis was then applied to the short-duration adverse weather scenarios for the two data sources in combination, to quantify the extremity (i.e. the return period) of events, and how these may change in future warmer climates. This analysis provided a return level curve for each event type, a combination of region and time window, and global warming level of interest. For each event combination, the extreme value analysis model was conditioned on global mean surface temperature, which allowed for the extremity of the event (maximum change in capacity factor) associated with a return level of interest (e.g. 1 in 100 years) to be estimated for any given global mean surface temperature warming level. For example, allowing for insights such as: a 1 in 20 year return level event, over a 1-hour time window and the Offshore North region, in the current day climate (warming level 1.2°C above pre-industrial) is expected to have a maximum change in wind generation capacity factor of 29.5 – 33.

Extreme value analysis model structures were tested and validated, and the final models, based on the best fitting model structure, were found to produce results consistent with those in the initial exploration of the short-duration adverse weather scenarios. The results of the statistical extreme value analysis were then used to select relevant short-duration adverse weather scenarios to represent each event combination. From these results it was determined that there was not a material difference in the return levels of each event type at the different warming levels which were investigated, and so it was decided that scenarios identified as

representative of the current warming level would be shared as these were shown to also be relevant for the future climate. Up to 10 short-duration adverse weather scenarios were then randomly sampled from those within the UKCP18 record characterising the associated return level range (e.g. a maximum change in wind generation capacity factor between 29.5 and 33).

Finally, the short-duration event addition to the 'Adverse Weather Scenarios for Future Electricity Systems' dataset was summarised and a brief how-to guide on downloading the data from the CEDA archive was included.

This study has provided a consistent approach for identifying, characterising and quantifying short-duration adverse weather scenarios for highly-renewable electricity systems without assuming a specific system. Hence the resulting short-duration subset of the 'Adverse Weather Scenarios for Future Electricity Systems' dataset can be used to test the resilience of a range of potential future electricity systems to large, short-term fluctuations in weather. This will enable energy system decision makers to support the security of energy supply as the UK becomes net-zero.

6 References

- Brown, S. J., Murphy, J. M., Sexton, D. M. H., and Harris, G. R. (2014). Climate projections of future extreme events accounting for modelling uncertainties and historical simulation biases. *Climate Dynamics*, 43(9-10):26812705.
- Burton, T., Sharpe, D., Jenkins, N., and Bossanyi, E., 2011. *Wind Energy Handbook*, Second Edition. Wiley, Chichester, West Sussex, UK.
- Butcher, T. and Dawkins, L. (2020). Adverse weather scenarios for renewable energy system testing: Discovery phase. Technical report.
- Cannon, D., Brayshaw, D., Methven, J., Coker, P. and Lenaghan, D., (2015). Using reanalysis data to quantify extreme wind power generation statistics: A 33 year case study in Great Britain, *Renewable Energy*, 75:767-778.
- Cannon, A. J., 2018. Multivariate quantile mapping bias correction: an N-dimensional probability density function transform for climate model simulations of multiple variables. *Climate Dynamics*, 50:31– 49.
- Climate Change Committee, 2020. Sixth Carbon Budget. Technical report.
- Coles, S., 2001. *An Introduction to Statistical Modeling of Extreme Values*. Springer.
- Dawkins, L., 2019. Weather and climate related sensitivities and risks in a highly renewable UK energy system: A literature review. Technical report.
- Dawkins, L. and Rushby, I., 2021. Characterising adverse weather for the UK electricity system, including addendum for surplus generation events. Technical report.
- Dawkins, L., Rushby, I., Pearce, M., Wallace, E. and Butcher, T., 2021a. Adverse Weather Scenarios for Future Electricity Systems. NERC EDS Centre for Environmental Data Analysis. Available at: <https://catalogue.ceda.ac.uk/uuid/7beed0bc7fa41feb10be22ee9d10f00>
- Dawkins, L., Rushby, I. and Pearce, M., 2021b. Adverse Weather Scenarios for Future Electricity Systems: Developing the dataset of long-duration events. Technical report.
- Dunstan, T., Lock, A., and Skea, A., 2016. Empirical error correction and feature identification for long term wind resource assessment using support vector regression. *Journal of Renewable and Sustainable Energy*, 8(013305).
- International Energy Agency, 2021. Net Zero by 2050: A Roadmap for the Global Energy Sector. Technical report.

Kendon, E., Short, C., Pope, J., Chan, S., Wilkinson, J., Tucker, S., Bett, P., Harris, G., 2021. Update to UKCP Local (2.2km) projections. Technical report.

Lowe, J. A. et al., 2018. UKCP18 science overview report. Technical report.

Murphy, J. M. et al. (2018). UKCP18 Land Projections: Science Report, November 2018. Technical report, Met Office.

National Infrastructure Commission, 2018. National Infrastructure Assessment. Technical report.

Pearce, M., Dawkins, L. and Rushby, I., 2021. Adverse Weather Scenarios for Future Electricity Systems: Characterising short-duration ramping events (including addendum). Technical report.

Smith, R. L., & Weissman, I. (1994). Estimating the Extremal Index. *Journal of the Royal Statistical Society. Series B (Methodological)*, 56(3), 515–528.

Watson, S., 2014. Quantifying the variability of wind energy. *Wiley Interdisciplinary Reviews - Energy and Environment*, 3(4):330–342.

7 Glossary

CEDA = Centre for Environmental Data Analysis

CDD = Cooling Degree Days

CF = Capacity Factor

Δ CF = Change in Capacity Factor

EVA = Extreme Value Analysis

GB = Great Britain

HDD = Heating Degree Days

IEC = International Electrotechnical Commission

MERRA = Modern-Era Retrospective analysis for Research and Applications

NEWA = New European Wind Atlas

SGI = Surplus Generation Index

UKCP18 = United Kingdom Climate Projections 2018

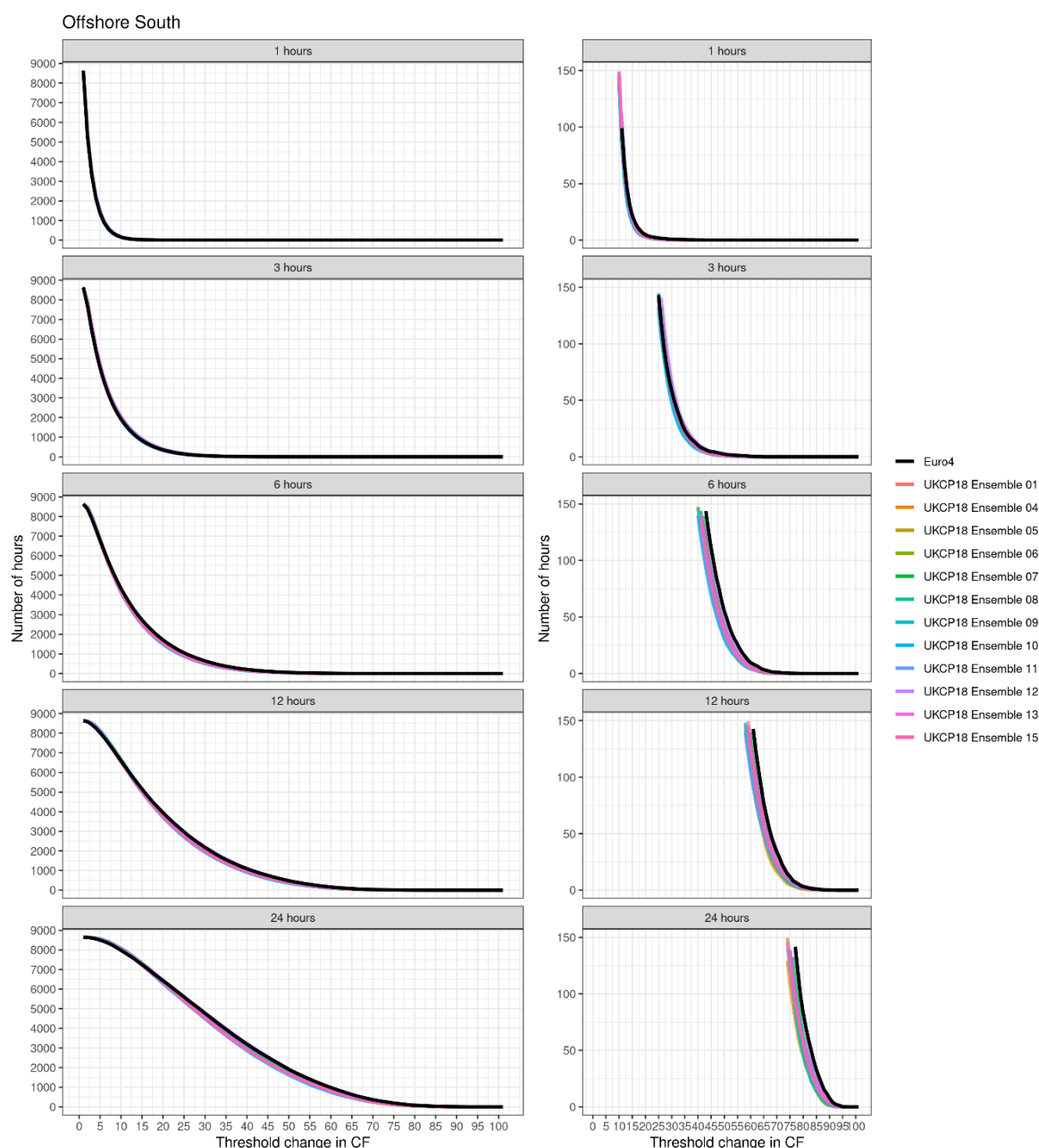
WDD = Weather Dependent Demand

WDI = Wind Drought Index

8 Appendix

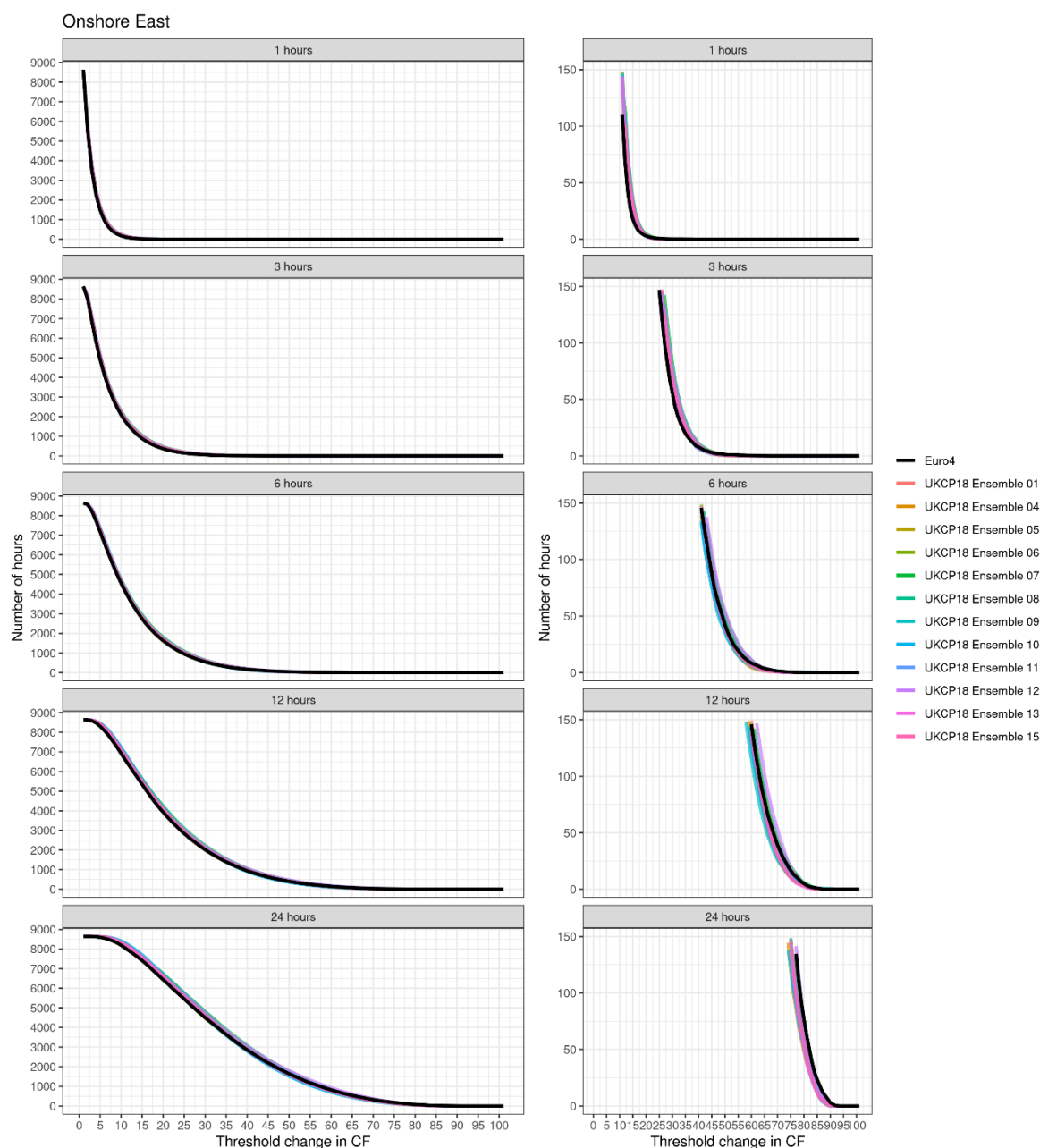
Appendix 1

The number of hours in an average year (y-axis) that a ramp event is observed reaching or exceeding a threshold of ΔCF (x-axis), for the Offshore South region. The black lines represent the Euro4 data and each of the other coloured lines on the plot represent a different UKCP18 ensemble member with a row per time window (1-, 3-, 6-, 12- and 24- hour time windows) identified in the top grey bar. The right-hand panel presents an exploration of the less frequent ramping events for each time window i.e., focusing on events reaching a threshold change less than 150 times (number of hours) in an average year between 1981 and 2000.



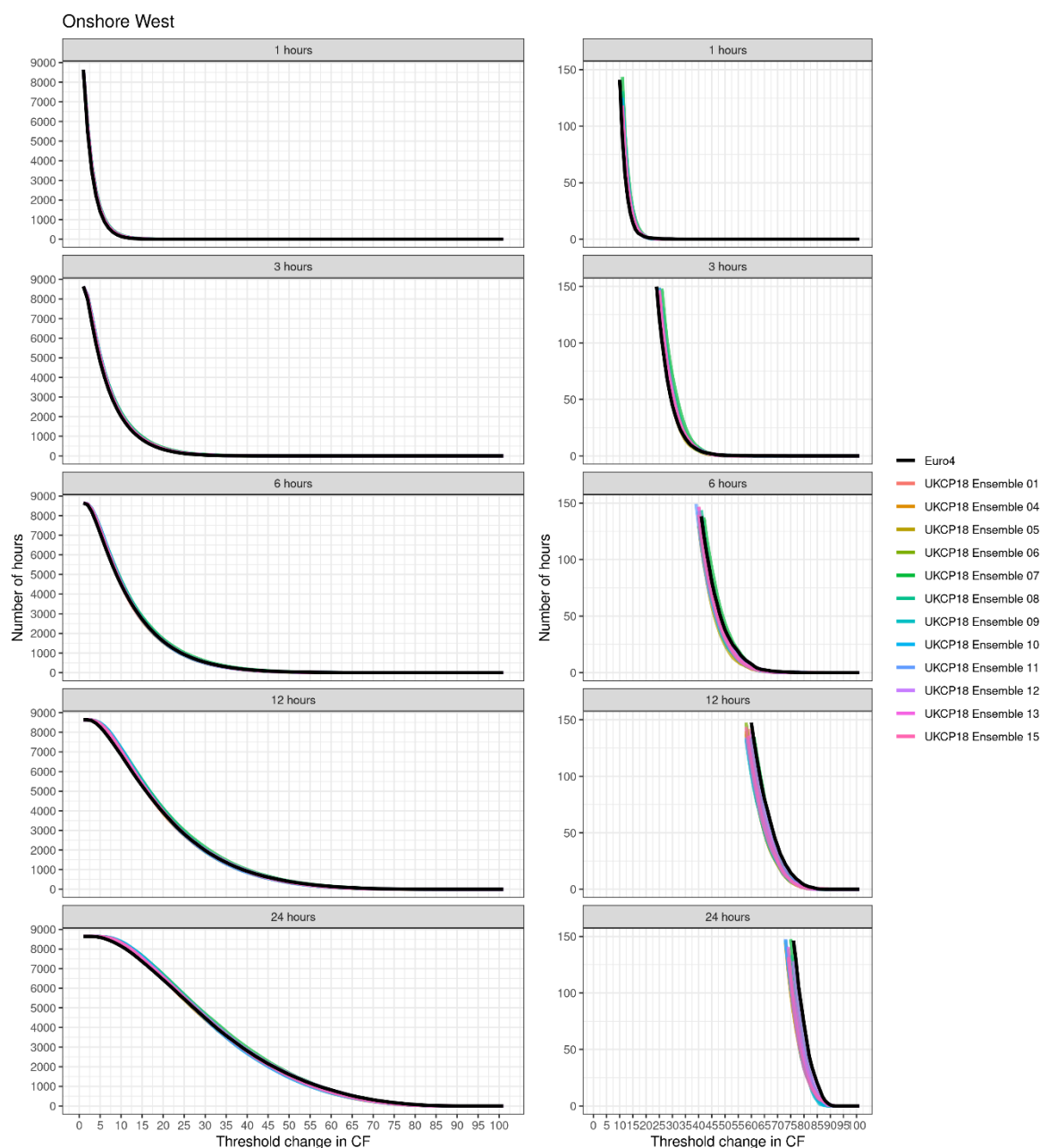
Appendix 2

The number of hours in an average year (y-axis) that a ramp event is observed reaching or exceeding a threshold of ΔCF (x-axis), for the Onshore East region. The black lines represent the Euro4 data and each of the other coloured lines on the plot represent a different UKCP18 ensemble member with a row per time window (1-, 3-, 6-, 12- and 24- hour time windows) identified in the top grey bar. The right-hand panel presents an exploration of the less frequent ramping events for each time window i.e., focusing on events reaching a threshold change less than 150 times (number of hours) in an average year between 1981 and 2000.



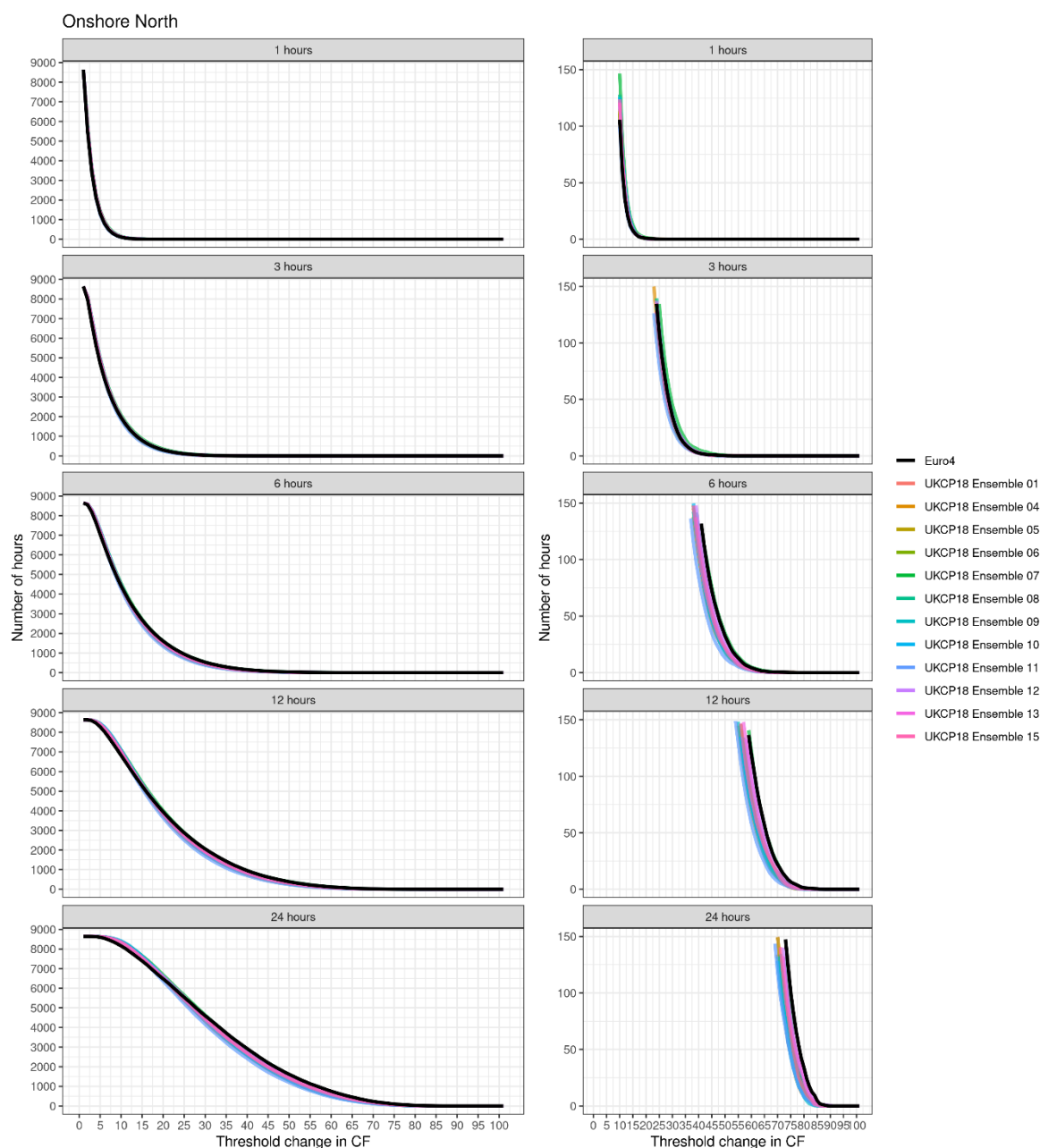
Appendix 3

The number of hours in an average year (y-axis) that a ramp event is observed reaching or exceeding a threshold of ΔCF (x-axis), for the Onshore West region. The black lines represent the Euro4 data and each of the other coloured lines on the plot represent a different UKCP18 ensemble member with a row per time window (1-, 3-, 6-, 12- and 24- hour time windows) identified in the top grey bar. The right-hand panel presents an exploration of the less frequent ramping events for each time window i.e., focusing on events reaching a threshold change less than 150 times (number of hours) in an average year between 1981 and 2000.



Appendix 4

The number of hours in an average year (y-axis) that a ramp event is observed reaching or exceeding a threshold of ΔCF (x-axis), for the Onshore North region. The black lines represent the Euro4 data and each of the other coloured lines on the plot represent a different UKCP18 ensemble member with a row per time window (1-, 3-, 6-, 12- and 24- hour time windows) identified in the top grey bar. The right-hand panel presents an exploration of the less frequent ramping events for each time window i.e., focusing on events reaching a threshold change less than 150 times (number of hours) in an average year between 1981 and 2000.



Appendix 5

```
#####  
#####  
README file to explain naming convention and file structure in the 'The Adverse  
Weather Scenarios for Future Electricity Systems' data set  
#####  
#####
```

The first set of directories represent the two categories of adverse weather scenario contained within the dataset:

1. Long duration events (long_duration_events)
2. Short duration events (short_duration_events)

```
#####  
#####  
Long duration events  
#####  
#####
```

The long duration component of the dataset contains time slices of surface temperature (tas), 100m wind speed (windspeed) and surface solar radiation (ssr), containing adverse weather scenarios for future electricity systems.

The first set of directories within the long_duration_events subdirectory represent the three forms of long duration adverse weather scenario considered:

1. Winter-time wind-drought-peak-demand events (winter_wind_drought)
2. Summer-time wind-drought-peak-demand events (summer_wind_drought)
3. Summer-time surplus renewable generation events (summer_surplus_generation)

Next, the region over which the adverse weather scenario is defined is selected:

1. UK only (uk)
2. Europe as a whole (europe)

Note: UK only events are those that are identified as impacting the UK, but meteorological data for all of Europe are still provided.

Following this, the return period of interest is selected (i.e. how often the adverse weather scenario is expected to occur on average). Adverse weather scenarios are available for 6 different return periods, as well as the three most extreme events in the historical DePreSys hindcast record for that event type:

1. 1 in 2 year (return_period_1_in_2_years)
2. 1 in 5 year (return_period_1_in_5_years)
3. 1 in 10 year (return_period_1_in_10_years)
4. 1 in 20 year (return_period_1_in_20_years)
5. 1 in 50 year (return_period_1_in_50_years)
6. 1 in 100 year (return_period_1_in_100_years)
7. Most extreme events (most_extreme_events)

Next, the adverse weather scenario metric is selected, representing in what way the event is characterised, i.e. in terms of:

1. Duration (duration)
2. Severity (severity)

Following this, the global warming level of interest is selected:

1. Global warming level 1.2 degrees Celcius above pre-industrial level (gw112degC)
2. Global warming level 1.5 degrees Celcius above pre-industrial level (gw115degC)
3. Global warming level 2 degrees Celcius above pre-industrial level (gw12degC)
4. Global warming level 3 degrees Celcius above pre-industrial level (gw13degC)
5. Global warming level 4 degrees Celcius above pre-industrial level (gw14degC)

In each case, the number of global warming level directories depends how the event duration/severity changes at different global warming level, according to the statistical extreme value analysis (see accompanying reports for these results).

For example, for winter-time wind-drought-peak-demand events in the UK with a return period of 1 in 20 years in terms of duration, events are found to be consistent

across all global warming levels. This directory is therefore expressed as 'gwl12-4degC'.

Conversely, for summer-time wind-drought-peak-demand events in Europe with a return period of 1 in 20 years in terms of duration, events are found to differ when the global warming level exceeds 1.5 degrees Celcius. These directories are therefore expressed as 'gwl12-15degC', 'gwl2degC', 'gwl3degC' and 'gwl4degC'.

Finally, the event number is chosen. In most cases three adverse weather scenarios/events are provided (selected from the DePreSys hindcast as described in the accompanying reports):

1. Event 1 (event1)
2. Event 2 (event2)
3. Event 3 (event3)

In some cases, where only two events exist within the DePreSys hindcast at the extreme level of interest, just these two events are provided. In the small number of cases where the DePreSys hindcast does not contain any events at the extreme level of interest, one event is provided from the UKCP18 global projections.

Each of the event directories then contains the gridded meteorological data associated with the adverse weather event. Each adverse weather scenario is contained within a time slice of data. For summer-time events, one calendar year (January - December) of data is provided, with the summer-time event occurring in the summer of that year. For winter-time events, two calendar years of data are provided, with the winter-time event occurring in the winter (October-March) intersecting the two calendar years. This data is provided for surface temperature (tas), 100m wind speed (windspeed) and surface solar radiation (ssr).

The directory route to the first event representative of a winter-time wind-drought-peak-demand adverse weather scenario in the UK with a return period of 1 in 20 years in terms of duration and all global warming levels is therefore:

winter_wind_drought/uk/return_period_1_in_20_years/duration/gwl12-4degC/event1/

And contained within this directory are three NetCDF files, each containing meteorological data for the same time slice but for each of the three meteorological variables:

1. winter_wind_drought_uk_return_period_1_in_20_years_duration_gwl12-4degC_event1_ssr.nc (surface solar radiation)
2. winter_wind_drought_uk_return_period_1_in_20_years_duration_gwl12-4degC_event1_tas.nc (surface temperature)
3. winter_wind_drought_uk_return_period_1_in_20_years_duration_gwl12-4degC_event1_windspeed.nc (wind speed at 100m height)

The metadata within each of these NetCDF files describes the data dimensions, details about the available variables, and global attributes describing the event specification (as described above), and the start date, duration and severity of the adverse weather scenario contained within the time slice of data.

For example, the metadata from the file 'winter_wind_drought/uk/return_period_1_in_20_years/duration/gwl12-4degC/event1/winter_wind_drought_uk_return_period_1_in_20_years_duration_gwl12-4degC_event1_tas.nc' looks like this:

```
netcdf classic {
  dimensions:
    longitude = 85 ;
    latitude = 81 ;
    time = 731 ;
  variables:
    NC_DOUBLE longitude(longitude) ;
    NC_CHAR longitude:units = "degrees_east" ;
    NC_CHAR longitude:long_name = "longitude" ;
    NC_DOUBLE latitude(latitude) ;
    NC_CHAR latitude:units = "degrees_north" ;
```

```

        NC_CHAR latitude:long_name = "latitude" ;
    NC_DOUBLE time(time) ;
        NC_CHAR time:units = "hours since 1970-01-01 00:00:00" ;
        NC_CHAR time:long_name = "time" ;
    NC_DOUBLE t2m(longitude, latitude, time) ;
        NC_CHAR t2m:units = "K" ;
        NC_DOUBLE t2m:_FillValue = NaN ;

// global attributes:
    NC_CHAR :Project = "Adverse weather scenarios for electricity systems
&€" Met Office, National Infrastructure Commition and Climate Change Committee" ;
        NC_CHAR                :Event                specification                =
"winter_wind_drought_uk_return_period_1_in_20_years_duration_gwl12-4degC" ;
    NC_CHAR :Event start date = "2012-02-18" ;
    NC_CHAR :Event duration = "13 days" ;
    NC_CHAR :Event severity = "7.17 (no units)" ;
    NC_CHAR :Domain = "Europe" ;
    NC_CHAR :Resolution = "60km" ;
    NC_CHAR :Frequency = "daily" ;
    NC_CHAR :Calendar = "gregorian" ;
    NC_CHAR :Meteorological variable = "Surface air temperature" ;
    NC_CHAR :Originating data source = "DePreSys" ;
}

```

```

#####
#####
Short duration events
#####
#####

```

The short duration component of the dataset contains time slices of 100m wind speed (windspeed), containing adverse weather scenarios for future electricity systems.

The subdirectory `wind_ramping_events` within the `short_duration_events` directory represents wind ramping events

Next, the region over which the adverse weather scenario is defined is selected:

- 1) Offshore North GB (`offshore_north_gb`)
- 2) Offshore South GB (`offshore_south_gb`)
- 3) Onshore North GB (`onshore_north_gb`)
- 4) Onshore East GB (`onshore_east_gb`)
- 5) Onshore West GB (`onshore_west_gb`)

Note: Events are those that are identified as impacting specific regions, but for each of the regions meteorological data covering the UK (land and offshore) are still provided.

Following this, the return period of interest is selected (i.e. how often the adverse weather scenario is expected to occur on average). Adverse weather scenarios are available for 6 different return periods:

1. 1 in 2 year (`return_period_1_in_2_years`)
2. 1 in 5 year (`return_period_1_in_5_years`)
3. 1 in 10 year (`return_period_1_in_10_years`)
4. 1 in 20 year (`return_period_1_in_20_years`)
5. 1 in 50 year (`return_period_1_in_50_years`)
6. 1 in 100 year (`return_period_1_in_100_years`)

Finally, the event number is chosen. In most cases 10 adverse weather scenarios/events are provided (selected from the UKCP18 dataset as described in the accompanying reports):

1. Event 1 (`event1`)
2. Event 2 (`event2`)
3. Event 3 (`event3`)
- ...
10. Event 10 (`event10`)

In some cases, where less than 10 events exist within the UKCP18 at the extreme level of interest, just these (between 5 and 9) events are provided. There are six event type and extreme level combinations where this is the case.

These events are:

- 11 in 100 year, 1-hour, Onshore East events (6 examples)
- 1 in 100 year, 1-hour, Offshore South events (9 examples)
- 1 in 100 year, 6-hour, Onshore East events (9 examples)
- 1 in 100 year, 12-hour, Onshore North events (5 examples)
- 1 in 100 year, 12-hour, Onshore West events (9 examples)
- 1 in 50 year, 24-hour, Onshore North events (9 examples)

Each of the event directories then contains the gridded meteorological data associated with the adverse weather event. This data is provided for 100m wind speed (windspeed). Each adverse weather scenario is contained within a time slice of data of up to 15 days.

For most events, the time slice contains 7 days before the day on which the event occurs, and 7 days afterwards.

However if the event occurs in within the first or last 7 days of each 20 year period of the UKCP18 dataset, all of the available data within these 15 days will be shared instead.

The events where this applies are:

- 1 in 20 year, 1-hour, Offshore South event 3
- 1 in 5 year, 3-hour, Onshore West event 8
- 1 in 10 year, 6-hour, Onshore North event 2
- 1 in 2 year, 6-hour, Offshore North event 8

The directory route to the first event representative of a 24-hour wind ramping scenario in the Onshore West region, at a 1 in 20 year return level is therefore:

```
.../short_duration_events/  
/wind_ramping/offshore_north_gb/1_hour_window/1_in_100_years/event1
```

And contained within this directory is one NetCDF file:

wind_ramping_offshore_north_gb_1_hour_window_1_in_100_years_event1_windspeed.nc

The metadata within each of these NetCDF files describes the data dimensions, details about the available variables, and global attributes describing the event specification (as described above), and the start date, magnitude and direction (of the maximum change in capacity factor) of the adverse weather scenario contained within the time slice of data.

For example, the metadata from the file 'wind_ramping_offshore_north_gb_1_hour_window_1_in_100_years_event1_windspeed.nc' looks like this:

```
netcdf netcdf4 {  
  dimensions:  
    time = 360 ;  
    grid_latitude = 450 ;  
    grid_longitude = 370 ;  
    bnds = 2 ;  
  variables:  
    NC_DOUBLE wind_speed(grid_longitude, grid_latitude, time) ;  
      NC_CHAR wind_speed:standard_name = "wind_speed" ;  
      NC_CHAR wind_speed:units = "m.s-1" ;  
      NC_CHAR wind_speed:grid_mapping = "rotated_latitude_longitude" ;  
    NC_INT rotated_latitude_longitude ;  
      NC_CHAR rotated_latitude_longitude:grid_mapping_name =  
"rotated_latitude_longitude" ;  
      NC_DOUBLE rotated_latitude_longitude:longitude_of_prime_meridian = 0 ;  
      NC_DOUBLE rotated_latitude_longitude:earth_radius = 6371229 ;  
      NC_DOUBLE rotated_latitude_longitude:grid_north_pole_latitude = 41 ;  
      NC_DOUBLE rotated_latitude_longitude:grid_north_pole_longitude = 193 ;  
      NC_DOUBLE rotated_latitude_longitude:north_pole_grid_longitude = 0 ;  
    NC_DOUBLE time(time) ;  
      NC_CHAR time:axis = "T" ;  
      NC_CHAR time:units = "hours since 1970-01-01" ;  
      NC_CHAR time:standard_name = "time" ;  
      NC_CHAR time:long_name = "time" ;
```

```

        NC_CHAR time:calendar = "360_day" ;
NC_FLOAT grid_latitude(grid_latitude) ;
        NC_CHAR grid_latitude:axis = "Y" ;
        NC_CHAR grid_latitude:bounds = "grid_latitude_bnds" ;
        NC_CHAR grid_latitude:units = "degrees" ;
        NC_CHAR grid_latitude:standard_name = "grid_latitude" ;
NC_FLOAT grid_latitude_bnds(bnds, grid_latitude) ;
NC_FLOAT grid_longitude(grid_longitude) ;
        NC_CHAR grid_longitude:axis = "X" ;
        NC_CHAR grid_longitude:bounds = "grid_longitude_bnds" ;
        NC_CHAR grid_longitude:units = "degrees" ;
        NC_CHAR grid_longitude:standard_name = "grid_longitude" ;
NC_FLOAT grid_longitude_bnds(bnds, grid_longitude) ;

// global attributes:
        NC_CHAR :Calendar = "360-day" ;
        NC_CHAR :Change in capacity factor = "38.11 (no units)" ;
        NC_CHAR :Direction of change = "Decreasing" ;
        NC_CHAR :Domain = "UK" ;
        NC_CHAR :Event number = "event1" ;
        NC_CHAR :Event region = "offshore_north_gb" ;
        NC_CHAR :Event specification =
"wind_ramping_offshore_north_gb_1_hour_window_1_in_100_years_event1" ;
        NC_CHAR :Event start date = "2069-11-27 11:00:00" ;
        NC_CHAR :Event window = "1_hour_window" ;
        NC_CHAR :Frequency = "Hourly" ;
        NC_CHAR :Height = "Equivalent to 100m" ;
        NC_CHAR :Originating data source = "UKCP18" ;
        NC_CHAR :Project = "Adverse weather scenarios for electricity systems
Met Office, National Infrastructure Commission and Climate Change Committee" ;
        NC_CHAR :Resolution = "4km" ;
        NC_CHAR :Return period = "1_in_100_years" ;
        NC_CHAR :Conventions = "CF-1.7" ;
}

```